Int J Comput Vis (2009) 83: 30–56
DOI 10.1007/s11263-009-0210-8

Replicator Dynamics in the Iterative Process for Accurate Range Image Matching

Yonghuai Liu

Received: 8 July 2008 / Accepted: 7 January 2009 / Published online: 3 February 2009

Abstract Iterative algorithms are often used for range image matching. In this paper, we treat the iterative process of range image matching as a live biological system: evolving from one generation to another. Whilst different generations of the population are regarded as range images captured at different viewpoints, the iterative process is simulated using time. The well-known replicator equations in theoretical biology are then adapted to estimate the probabilities of possible correspondences established using the traditional closest point criterion. To reduce the effect of image resolutions on the final results for efficient and robust overlapping range image matching, the relative fitness difference (rather than the absolute fitness difference) is employed in the replicator equations in order to model the probability change of possible correspondences being real over successive iterations. The fitness of a possible correspondence is defined as the negative of a power of its squared Euclidean distance. While the replicator dynamics penalize those individuals with low fitness, they are further penalised with a parameter, since distant points are often unlikely to represent their real replicators. While the replicator equations assume that all individuals are equally likely to meet each other and thus treat them equally, we penalise those individuals competing for the same points as their possible replicators. The estimated probabilities of possible correspondences being real are finally embedded into the powerful deterministic annealing scheme for global optimization, resulting in the camera motion parameters being estimated in the weighted least squares sense. A comparative study based on real range images with partial overlap has shown that the proposed algorithm is promising for automatic matching of overlapping range images.

Keywords Replicator dynamics · Iterative process · Accurate matching · Overlapping range images · Fitness · Probability of a possible correspondence being real

Y. Liu (✉)
Department of Computer Science, Aberystwyth University, Ceredigion SY23 3DB, Wales, UK
e-mail: yyl@aber.ac.uk

1 Introduction

The latest laser range scanners have become more and more popular for 3D measurement. The output of laser range scanners is a set of structured data points with or without reflectance strength information, depicting the reflectance characteristics of the 3D objects of interest. The structured data points can easily be triangulated and rendered as range images (Fig. 1). These range images are described in local camera-centred coordinate systems. Accurate matching of overlapping range images finds numerous applications of the latest laser scanning techniques in areas such as image recognition, image retrieval, image transmission, object modelling, simultaneous localization and map building (SLAM), and industrial inspection. Range image matching has two goals: one is to establish correspondences between overlapping range images, and the other is to estimate the camera motion parameters that bring one range image into the best possible alignment with the other. Fixing one goal renders the other trivial.

1.1 Previous Work

Due to the challenging nature of automatic range image matching, a large number of algorithms have been developed. In Besl and McKay (1992), Zhang (1992), the closest

points in one range image to the transformation of points in another are selected as possible correspondences. When the surface represented by one range image is a subset of that represented by another, there is no need for too much concern over outliers, due mainly to noisy points, occlusion, appearance and disappearance of points in different range images. Otherwise, if the distance between a possible correspondence is larger than a threshold, then it should be regarded as an outlier. A scheme for dynamically setting up this threshold is proposed in Zhang (1992). While the sum of the squared distances between possible correspondences is minimized for the camera motion estimation in Besl and McKay (1992), Zhang (1992), it is proposed in Chen and Medioni (1992) to minimise the sum of the squared distances from the transformation of points in one range image to the tangent planes at the intersection points between the normals at the transformed points and the surface represented by another. The algorithm proposed in Besl and McKay (1992), Zhang (1992), Chen and Medioni (1992) is usually collectively called the iterative closed point (ICP) algorithm. The ICP algorithm has attracted intensive attention from 3D imaging community and has become a standard approach for range image matching. Its brief analysis is given in the next section. In Gold et al. (1998), Dewaele et al. (2004), the probabilities of possible correspondences as a complete combination of all the points in the two images being matched are estimated through maximizing the entropy of these probabilities. While a two-way constraint is imposed to refine the probabilities of possible correspondences in Gold et al. (1998), a one-way constraint is imposed instead in Dewaele et al. (2004). In Liu (2005, 2006), it is proposed to consider the closest points for efficient registration, instead of the complete combination of all the points in the two images being matched.

In Johnson and Hebert (1999), spin images are firstly extracted for the representation of the points in different images and then matched for the establishment of possible correspondences between the images being registered. To eliminate false correspondences, a geometric consistency test is performed with regard to the similarity measure between two spin images and the discrepancy between the spin-map coordinates. Spin images are chosen in Huber and Hebert (2003) for pair-wise registration of data sets in the process of automatic registration of multiple data sets. Overlapping distance, free space violation fraction, and free space violation odds are defined between two registered surfaces and are used to rank the results of pair-wise matching. While the dimensionality of spin images (Johnson and Hebert 1999) is two, the information in Brusco et al. (2005) used for creating the spin image histogram is three dimensional with axes representing the grey level value as a function of chromatic values (R, G, B) of the surface texture and the distances of any neighbouring point from and along the normal vector at the point of the interest. The dimensionality of the spin image depends on the number of features used to encapsulate the local geometric and/or optical information for the representation of points. The size of the spin image depends on the spatial quantization of these features. After surfaces have been represented as triangular meshes, the including angle between a facet of interest and any of its neighbours within a certain distance and the weighted distance from all the points in the neighbouring facet to the plane that contains the facet of interest are used in Ashbrook et al. (1998) to construct a 2D frequency histogram, where the weight is computed as the product of the areas of the two facets. Through matching the frequency histograms from two surfaces, facet correspondences are established and applied to estimate the transformation for the alignment of the two surfaces using the Hough accumulator. In Xiao et al. (2007), signed distance vectors are computed in 3D volumetric space for each voxel and matched using dynamic programming, yielding corresponding voxel pairs, from which a list of candidate transformations is estimated and optimized by minimizing the sum of residuals of corresponding surface voxels. A 2D histogram about the 3D shape index and the including angle between the normal vector at a point of interest and that of its neighbour is constructed in Chen and Bhanu (2007) for the representation and matching of the points of interest with the final results being refined using a ICP variant (Zhang 1992). In Chang et al. (2004), a medial scaffold graph is extracted from each 3D shape and matched against that from another using the graduated assignment algorithm (Gold and Rangarajan 1996). In Makadia et al. (2006), the constellation image is extracted from each range scan. To deal with the computational efficiency, the spherical harmonics and the rotational Fourier transform of these constellation images are computed. The camera rotation parameters are estimated as those maximizing the correlation of the transformed constellation images from two range scans, while the camera position parameters are estimated as those maximizing the convolution of the occupancy grid of one range scan and the shifted occupancy grid of another.

In Lomonosov et al. (2006), a genetic search algorithm (GA) is used to pre-register two overlapping surfaces. This algorithm encodes 7 parameters as integers: one for overlap, three for Euler angles of camera rotation and three for camera position, and minimizes the trimmed mean of squared errors of possible correspondences divided by a power of the overlap. It is proposed in Silva (2005) that in the beginning iterations of registration, the GA minimizes the mean of squared errors of possible correspondences with outliers rejected by a threshold, while in the later iterations it maximizes the surface interpenetration measure (SIM). The hill-climbing offset range for the generation of a new candidate solution to each of the six parameters, three for camera rotation and three for camera position, is dynamically decreased.

Instead of randomly selecting and combining the candidate solutions, the scatter search (Santamaria et al. 2007) adopts for computational efficiency a complete combination of all the possible solutions in a reference set whose size is much smaller than that of the population as in the traditional GA. To combine different solutions, the BLX_α method is employed.

The aforementioned *automatic* range image matching algorithms can be classified into three main categories: (1) feature extraction and matching (Johnson and Hebert 1999; Huber and Hebert 2003; Brusco et al. 2005; Ashbrook et al. 1998; Chang et al. 2004), (2) iterative possible correspondence establishment and camera motion estimation from these possible correspondences (Besl and McKay 1992; Zhang 1992; Chen and Medioni 1992), and (3) iterative camera motion search and evaluation of the resulting camera motion parameters (Lomonosov et al. 2006; Silva 2005; Santamaria et al. 2007). All these approaches have their own advantages and disadvantages and could succeed in one situation, but degrade catastrophically in another. Feature extraction and matching approaches are susceptible to outliers and common ambiguities Makadia et al. (2006). The establishment of possible correspondences and camera motion parameter re-estimation from these possible correspondences are interwoven (Gold et al. 1998) and require an accurate initialization of camera motion parameters. Iterative camera motion search requires prior knowledge about range and desired accuracy of the camera motion parameters and is usually computationally intensive. Consequently, automatic range image matching still remains a major hurdle in 3D data acquisition (Zagorchev and Goshtasby 2005).

1.2 Brief Analysis of ICP

The ICP algorithm has become a standard approach for range image matching. However, it introduces false correspondences in almost every iteration of the matching for the following reasons.

1. Occlusion, appearance and disappearance of points in different range images are almost always present.
2. The imaging process introduces noise due to point sampling on the object surface, measurement quantization, electrical and mechanical errors, shape discontinuities, and various reflectance properties of the object surface.
3. A single distance constraint is employed to determine the correspondent of a point and a single constraint in general cannot uniquely determine the exact position of a point in 3D space.
4. The initial camera motion parameters are not necessarily very accurate. Even though they are relatively accurate, they cannot guarantee that the ICP algorithm will always produce more accurate camera motion parameter estimation results (Brusco et al. 2004). While the matching objective function is a complex non-linear function of camera motion parameters and may have a large number of local optima determined by the actual range images being matched, the iterative optimization procedure in the ICP algorithm cannot guarantee that the global optimum of the matching objective function is always found.

As a result, a large number of ICP variants have been proposed for more accurate and robust matching results based on techniques such as removing boundary points (Turk and Levoy 1994); using rigid motion constraints (Liu et al. 2000) or collinearity constraints (Liu et al. 2006a); combining rigid motion constraints with structural constraints (Liu and Wei 2004); checking the interpoint distance compatibility (Dorai and Wang 1998) or orientation consistency (Pulli 1999; Zhang 1992); increasing the dimensionality of points using invariant features (Sharp et al. 2002), colour (Schutz et al. 1998), or laser reflectance strength value (Allen et al. 2003); matching interpoint distances (Chen et al. 1999), 2D spin images (Andreetto et al. 2004; Huber and Hebert 2003; Johnson and Hebert 1999), textured 2D spin images (Brusco et al. 2005), or surface signatures (Yamany and Farag 2002); resampling points in the normal space (Rusinkiewicz and Levoy 2001); dynamically thresholding false correspondences (Zhao et al. 2004); using ϵ reciprocal points for the camera motion estimation (Pajdla and Van Gool 1995); bootstrapping camera motion models and transformation estimate (Stewart et al. 2003); and taking the confidence value of each point into account for camera motion estimation (Zhu et al. 2007).

In order to update the camera motion parameters, it is vital to evaluate the possible correspondences established. The existing evaluation methods can be classified into two main categories: (1) classify these correspondences into either real or false ones (Zhang 1992; Turk and Levoy 1994; Liu et al. 2000; Liu et al. 2006a; Pulli 1999), and (2) estimate the probabilities of these correspondences being real (Liu 2005; Liu 2006; Granger and Pennec 2002). While the first class of methods usually requires that the range images include objects with complex enough geometry so that reliable features can be extracted and employed to do the classification, the second class has to deal with outliers in one way or another and accurately estimate and globally optimize the probabilities of possible correspondences being real. The former has an advantage in being more computationally efficient, but often fails in the following two scenarios: (1) when the range images include objects either with symmetry or with relatively simple geometry such as spheres, cones, and cylinders; and (2) when extracted features are either too sensitive to imaging noise, occlusion, appearance and disappearance of points in any image or too inexpressive for the representation of the objects of interest

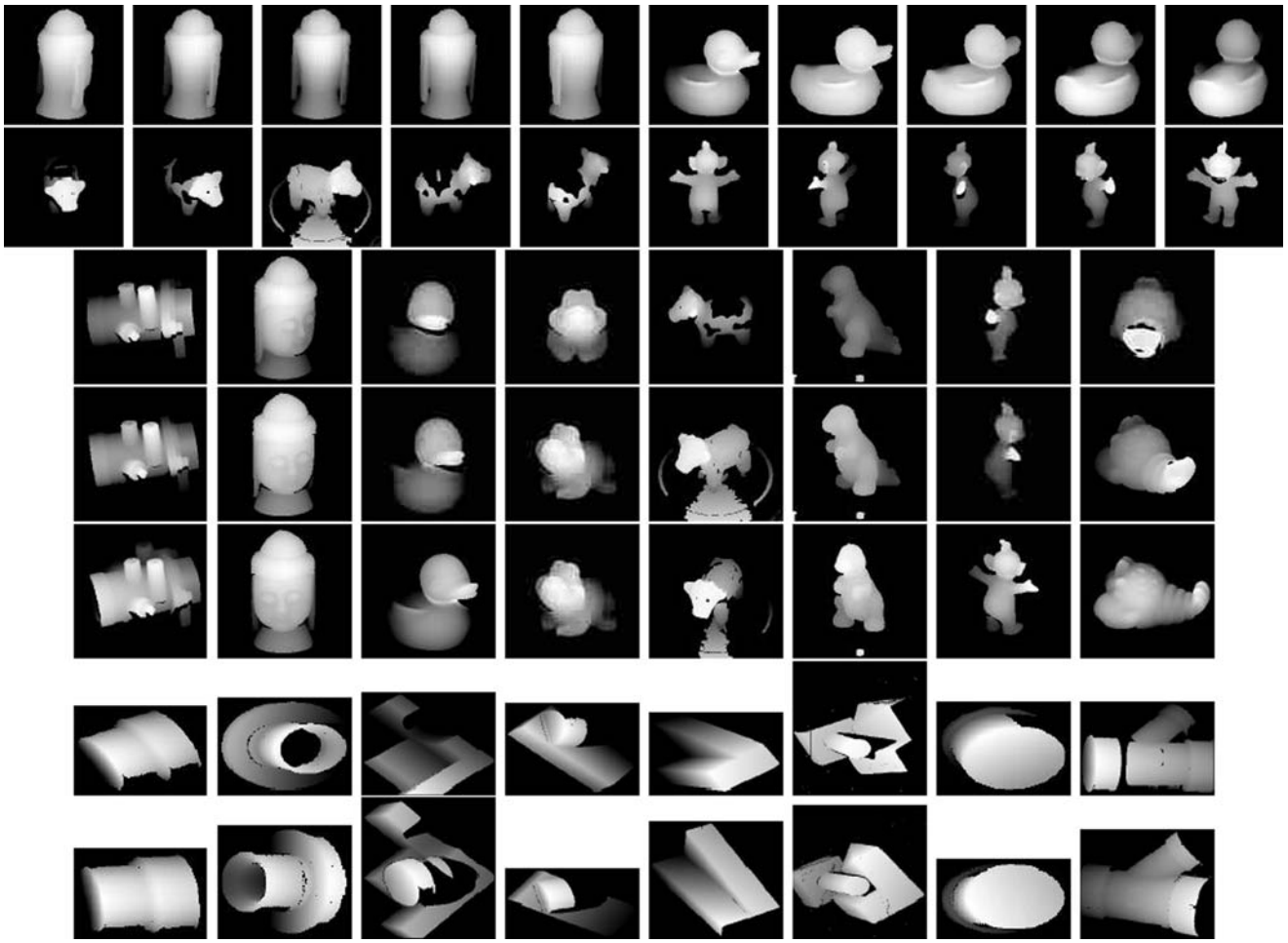

Fig. 1 Sample real range images used. Images in *top two rows* are used for training. The other images are used for performance test. From *top left* to *bottom right* in *top two rows*: buddha140, 160, 180, 200, and 220, duck160, 180, 200, 220, and 240, cow48, 51, 54, 57, and 60, and tubby180, 220, 260, 300, and 340. Images in *rows* 3, 4 and 5 from *left column* to *right column*: value0, 10, and 20, buddha40, 20, and 0, duck100, 120, and 140, frog40, 20, and 0, cow39, 42, and 45, dinosaur0, 36, and 72, tubby60, 100, and 140, and lobster60, 100, and 140. Images in *rows* 6 and 7 from *left column* and *right column*: adapter-2 and 3, agpart2-2 and 1, curvblock-2, adapter+curvblock, hump-3 and 1, block1-2 and 1, occl4 and 5, cap2 and 3, and bigwye3, and 4. The images in the *top* 5 *rows* were captured using a Minolta Vivid 700 range camera, while those in the *bottom two rows* were captured using a Technical Arts 100X range scanner

from different viewpoints. The latter has an advantage in being more robust and stable and producing accurate matching results, but often requires an explicit modelling of outliers and accurate estimation and optimization of the probabilities of possible correspondences being real.

1.3 Inspiration from Replicator Equations

Since the fundamental theorem of natural selection was first formulated by Fisher in his 1930 book (Fisher 1930), it has been intensively employed to investigate the dynamics of interactive game and biologically evolutionary processes (Novak and Sigmund 2004; Stadler and Stadler 2003). The fundamental theorem of natural selection (Fisher 1930) states that the rate of increase in fitness of any organism at any time is equal to its genetic variance in fitness at that time. It describes the evolution of a population in which, unless there is accidental mutation, the offspring will completely inherit the traits of their parents. All individuals behave according to pre-programmed patterns, that is, pure strategies.

In contrast, as far as we are aware, this useful principle has attracted little attention from the 3D imaging community. Careful analysis reveals that range image matching, interactive game and biological systems differ in the following six aspects.

1. While the replicator equations describe a pseudo-dynamic system whose payoff matrix is usually determined in advance, range image matching represents a truly dynamic system in which the fitness of each individual has to be re-estimated at each iteration.

2. While the replicator equations describe a process whose evolutionary behaviour is determined by the fixed payoff matrix, the trajectory of evolutionary range image matching process is determined by the target range image $\mathbf{P}'$ for the first range image $\mathbf{P}$ to evolve towards.
3. While the replicator equations assume that the individuals in the population can be selected multiple times, range image matching algorithms assume that each individual can only be selected at most once.
4. While the replicator equations assume that the individuals are completely mixed and thus are equally likely to meet each other, range image matching algorithms assume that closer points are more likely to be their replicators.
5. While the replicator equations assume that the individuals with low fitness will shrink, range image matching algorithms assume that such individuals can even be further penalized.
6. While the replicator equations treat all individuals equally, range image matching algorithms usually have to penalise those individuals that compete for the same points as their possible replicators.

Thus, the replicator equations have to be adapted so that they are applicable to accurate automatic range image matching. The adaptation, however, is not trivial.

It is believed that range image matching provides a perfect *platform* to test, understand and further develop the replicator equations for various real world applications, since the data can be easily captured for the verification of the theoretical analysis results using the latest laser range scanners within seconds. This is in sharp contrast with the fact that, when the replicator equations have been analysed in the context of interactive game and evolutionary biology, limited data is often used to validate system behaviour and only unsuitable incomplete ecological data is available.

1.4 The Proposed Work

In this paper, a novel automatic range image matching algorithm is developed. Range images are represented as point clouds captured using laser range scanners. The novelty of the proposed algorithm lies in that the replicator equations are adapted from the field of interactive game and mathematical biology for the modelling of the dynamics in the iterative process of automatic overlapping range image matching.

We regard the automatic iterative range image matching process as an evolutionary one. Thus, the replicator equations are applicable to the description of its dynamics. In this process, we consider that the population consists of all the points in one range image, and the relative frequency of each individual is defined as its normalized probability being in the overlapping area with another. The fitness of each individual is defined as a negative function of the squared Euclidean distance between its resulting possible correspondence in the two overlapping range images established using the traditional closest point criterion (CPC) (Besl and McKay 1992). The average fitness of the entire population is defined as the weighted average fitness over the entire population. While the replicator equations consider the absolute fitness difference, we consider the relative fitness difference instead in the replicator equations for the modelling of the probability change of each individual being in the overlapping area over successive iterations.

The replicator dynamics penalize those individuals with low fitness. We further penalise them using a parameter with an attempt to increase the average fitness of the entire population. While the replicator equations assume that different individuals are equally likely to meet each other and treat them equally, we penalise those individuals that compete for the same points in the target range image as their possible replicators, since they are unlikely to lie simultaneously in the overlapping area. The estimated probability of any individual being in the overlapping area is finally embedded into the powerful deterministic annealing scheme (Puzicha et al. 1997) for global optimization with an attempt to obtain accurate range image matching results. Since our algorithm is a novel variant of the traditional ICP algorithm (Besl and McKay 1992; Zhang 1992) and models the dynamics of the evolutionary overlapping range image matching process, it is called the EvolICP algorithm in the rest of this paper.

For a comparative study of performance, we duplicated the experimental results of the genetic algorithm (GA) in Silva (2005) and the feature extraction and matching of local surface patches (LSP) (Chen and Bhanu 2007) and implemented the extended version, SoftICP (Liu 2005; Liu 2006), of the SoftAssign algorithm (Gold et al. 1998) and the GenICP algorithm proposed in Liu et al. (2006b). These four algorithms were selected respectively from the three different classes of methods discussed above in Sect. 1.1 and represent the state of the art technique for automatic overlapping range image matching. The other reasons why the latter two algorithms were chosen for a comparative study are that:

- They are all extensions of the popular traditional ICP algorithm (Besl and McKay 1992; Zhang 1992), applying the same criterion to establish possible correspondences and then using various strategies for their evaluation. While the SoftICP algorithm applies the traditional Shannon entropy to estimate the probabilities of possible correspondences being real, the GenICP algorithm applies Tsallis entropy. They all have an advantage of easy implementation;
- The classification based ICP variants (Turk and Levoy 1994; Zhang 1992; Pulli 1999; Liu and Wei 2004; Rusinkiewicz and Levoy 2001) are usually not robust,

since it is often difficult for them to develop universally effective classification rules. In contrast, the probability based ICP variants (Liu 2005; Liu 2006; Liu et al. 2006b), as is the case for both the SoftICP and GenICP algorithms, often succeed in explicitly modelling outliers, applying the entropy maximization principle (Gold et al. 1998) for the estimation of the probabilities of possible correspondences being real, and globally optimizing them using the powerful deterministic annealing scheme (Puzicha et al. 1997) and thus, are generally more robust; and

- The dynamics these two algorithms describe in the iterative process for automatic overlapping range image matching is closely related to that the proposed EvolICP algorithm does. The actual relations are outlined in the next section.

Thus, such comparative study is interesting and valuable and can reveal which dynamic is more effective for the description of the iterative process for automatic overlapping range image matching.

While the CPC searches possible correspondences in the image space, the GA searches camera motion parameters in the camera motion space for overlapping range image matching. Such comparative study is again interesting, since it can reveal which strategy is more effective for automatic overlapping range image matching: either firstly search possible correspondences and then evaluate these correspondences for camera motion parameter re-estimation or firstly search camera motion parameters and then evaluate these parameters usually involving the resulting possible correspondences for camera motion optimization.

While the proposed EvolICP algorithm evolves the probabilities of possible correspondences being real, the LSP method directly identifies possible point matches. Such comparative study is again interesting, since it can reveal whether a closed form or iterative solution is more effective for the establishment of real correspondences.

1.5 Experimental Setup and Performance Measurement

The experiments carried out in this paper were based on 86 real range images all downloaded from a publicly available range image database currently hosted by the Signal Analysis and Machine Perception laboratory at Ohio State University. These images were captured using either a Minolta Vivid 700 range camera or a Technical Arts 100X range scanner and were represented as point clouds. 20 images captured using the Minolta Vivid 700 range camera were used to fine tune the parameters involved in the proposed EvolICP algorithm. Another 66 images were used for a comparative study of performance of different algorithms. All the images captured using the Minolta Vivid 700 range camera are named as the object name followed by the rotation angle of the camera motion. All the images captured using the Technical Arts 100X range scanner are named the same as those in the original database.

All experiments were performed on a Pentium IV, 2.80 GHz, 504 MB RAM computer using the programming language C within the MS visual C++ 6.0 package. The proposed EvolICP algorithm was always initialised by the pure translational motion derived from the centroid difference of the two point clouds being matched. It was directly applied to real range images without any image pre-processing or feature extraction and matching and also without any prior knowledge about the distribution of points, occlusion, appearance and disappearance of points in different images, or motion information. Thus, experiments based on such images are objective in revealing its performance for automatic overlapping range image matching.

To measure the performance of matching algorithms, the following parameters were defined: the average e_μ and standard deviation e_σ of matching errors in millimetres based on reciprocal correspondences (RCs), and the matching time in seconds. A RC is such a possible correspondence $(\mathbf{p}_i, \mathbf{p}'_{c(i)})$ between two overlapping range images $\mathbf{P}$ and $\mathbf{P}'$ that $\mathbf{p}_i$ in $\mathbf{P}$ finds $\mathbf{p}'_{c(i)}$ in $\mathbf{P}'$ as its possible correspondent and $\mathbf{p}'_{c(i)}$ in $\mathbf{P}'$ finds also $\mathbf{p}_i$ in $\mathbf{P}$ as its possible correspondent. In the figures of matching results, yellow colours represent the transformed first range images and green colours represent the second range images.

The rest of this paper is structured as follows: Sect. 2 briefly analyses the replicator equations and discusses the inherent relations amongst the EvolICP, SoftICP and GenICP algorithms in the sense of the dynamics they describe in the iterative process for overlapping range image matching. Section 3 develops the novel range image matching algorithm, while Sect. 4 presents the experimental results. Finally, Sect. 5 discusses a number of issues related to overlapping range image matching and draws some conclusions.

2 Brief Analysis of Replicator Equations

In this section, we briefly analyse the properties of the replicator equations that are useful for overlapping range image matching algorithm development. The following notations are used throughout this paper: capital letters denote vectors or matrices, lower case letters denote scalars, $\|\cdot\|$ denotes the Euclidean norm of a vector, $|\cdot|$ denotes the absolute value of a scalar, and parameters with and without $\hat{}$ denote estimated and real ones respectively. Two pairs of terms, (1) the fitness of an individual being in the overlapping area and the fitness of a possible correspondence being real, and (2) the normalized probability of a possible correspondence being real and the relative frequency of a point in

one range image being in the overlapping area with another, will be used interchangeably without causing any ambiguity in understanding the relative contents.

2.1 Properties of Replicator Equations

As early as 1930, R.A. Fisher proposed a well known theorem (Fisher 1930), called the fundamental theorem of natural selection. This theorem states that the rate of increase in fitness of any organism at any time is equal to its genetic variance in fitness at that time. Mathematically, this theorem can be represented as:

$$\dot{w}_i = w_i(e_i - E), \tag{1}$$

where $\dot{w}_i$ denotes the derivative with regard to time t of the relative frequency w_i of an individual i in the population, e_i is its fitness, and E is the weighted average fitness of the entire population. This equation describes the dynamics of natural selection. The state of the population at time t is described simply as a vector $\mathbf{w}(t) = \{w_1(t), w_2(t), \ldots, w_n(t)\}$ which is clearly constrained to lie in the standard simplex in the n-dimensional Euclidean space: $\mathbf{S}_n = \{\mathbf{w} \in \mathbf{R}^n : \sum_i w_i = 1,\ w_i \geq 0\}$.

Replicator equations make the following assumptions:

- Infinite population size: Assuming an infinitely large population makes the equations easier to understand and analyze, as the dynamics of populations become deterministic when an infinite number of individuals is assumed. In the case of a finite population size, the dynamics of populations become stochastic;
- Continuous time: The dynamics in a replicator equation are defined by the rates of birth and death of individuals, resulting in differential equations;
- Complete mixing: It is assumed that all individuals in the population have an equal chance to meet each other in a game to determine their interdependent payoff or fitness; and
- Strategies breed true: Strategies are assumed to be inherited into the next population dependent on their expected payoff.

While the assumptions of the replicator equations hold true to varying degrees in different situations, they find wide applications in interactive game theory and mathematical biology (Novak and Sigmund 2004; Stadler and Stadler 2003). In population genetics, the population represents all possible individuals. Let A_i denote the expected number of offspring from individual i. Then the payoff matrix of the population can be defined as: $\mathbf{U} = \{u_{ij} = A_i A_j\}$. In game theory, the population represents a set of available strategies. Let u_{ij} denote the payoff of playing strategy i against strategy j. Then the fitness of strategy i is: $e_i = \sum_j u_{ij} w_j$ and the weighted average fitness of the entire population is: $E = \sum_i \sum_j u_{ij} w_i w_j$. The replicator equation has the following appealing properties:

- The state vector $\mathbf{w}(t)$ always lies in the simplex $\mathbf{S}_n$ due simply to the fact that: $\sum_i \dot{w}_i = 0$. This means that the state vector always represents the relative frequency of each individual in the population;
- When $\mathbf{U} = \{u_{ij}\}$ is symmetric, then the weighted average fitness E of the entire population always increases over time;
- When $\mathbf{U} = \{u_{ij}\}$ is symmetric, the dot product of vectors $\mathbf{w}(t)$ and $\mathbf{U}\mathbf{w}(t)$ is a Lyapunov function. Thus, a system with the replicator dynamics is always stable; and
- If $\mathbf{w} \in \mathbf{S}_n$ is evolutionarily stable, then $\mathbf{w}$ is in asymptotical equilibrium. The converse is not valid. For $n \leq 3$, the replicator equation has no limit cycles. For $n \geq 4$, it has limit cycles for certain payoff matrices. If there is no fixed point in the interior of $\mathbf{S}_n$, then every trajectory converges to the boundary of $\mathbf{S}_n$. If, on the other hand, the boundary is repelling, then there exists a unique fixed point in the interior, which corresponds to the time average of every trajectory in the interior of $\mathbf{S}_n$.

The first property actually implements a normalisation of the state vector through the dynamics themselves; the second makes sure that under certain conditions, the system will improve its performance steadily over time; the third guarantees that under certain conditions, the evolutionary system is stable no matter where the system starts the evolution from; and the fourth reveals when there are optimal solutions and where these solutions are. All these properties are appealing for overlapping range image matching. The first property normalises the probabilities of possible correspondences required for the estimation of camera motion parameters; the second implies that the average matching error of the entire population is likely to monotonically decrease over successive iterations; the third implies that the final matching results have nothing to do with and thus greatly facilitate the initialization of the parameters of interest; and the fourth shows how to efficiently search the optimal state variables and how to evaluate the final state variables for camera motion estimation. When the system is stable: $\dot{w}_i = w_i(e_i - E) = 0$, then either $w_i = 0$ or $E = e_i$. The former implies that individual i dies and thus, is a disappearing point, while the latter implies that individual i survives and thus, is a point in the overlapping area. Although range image matching algorithms seek to possess all these appealing properties, the problem lies in how to establish their corresponding pre-conditions. While we *emphasise* the range image matching algorithm development in this paper, the theoretical investigation of these pre-conditions are left for our future research. These pre-conditions will help gain knowledge about the behaviour of the proposed EvolICP algorithm which is developed in the next section for automatic

overlapping range image matching: whether it will successfully evolve one range image towards another.

2.2 Inherent Relations amongst EvolICP, SoftICP, and GenICP

The SoftAssign algorithm (Gold et al. 1998) constructs the following objective function for free form shape matching:

$$E_{3D}(\mathbf{M},\mathbf{R},\mathbf{t}) = \min_{\mathbf{M},\mathbf{R},\mathbf{t}} \sum_{j=1}^{n_2}\sum_{i=1}^{n_1} m_{ij}\|\mathbf{p}'_j - \mathbf{R}\mathbf{p}_i - \mathbf{t}\|^2 - \alpha\sum_{j=1}^{n_2}\sum_{i=1}^{n_1} m_{ij} + \frac{1}{\beta}\sum_{j=1}^{n_2}\sum_{i=1}^{n_1} m_{ij}(\ln m_{ij} - 1). \quad (2)$$

This objective function simultaneously optimises the correspondence matrix $\mathbf{M} = \{m_{ij}\}$ ($m_{ij} \in [0,1]$) and the camera motion parameters rotation matrix $\mathbf{R}$ and translation vector $\mathbf{t}$. In this objective function, the first term is the matching error of a point match $(\mathbf{p}_i, \mathbf{p}'_j)$, the second term maximises the overlapping area between the free form shapes being matched, and the third term is a barrier function making sure that m_{ij} is positive.

Careful analysis reveals that the objective function equation (2) maximises the traditional Shannon entropy: $H_S = -\sum_j \sum_i m_{ij} \ln m_{ij}$. While the parameter α does not affect the estimation of m_{ij} due to normalization, the dynamic embedded in the objective function equation (2) can be described as:

$$\dot{m_{ij}} = -\beta m_{ij}\|\mathbf{p}'_j - \mathbf{R}\mathbf{p}_i - \mathbf{t}\|^2. \quad (3)$$

Comparing (1) with (3), it can be seen that they are very similar and the latter assumes that the weighted average fitness of the entire population is zero. Hence, the SoftAssign algorithm describes a special case of replicator dynamics.

While the SoftAssign algorithm applies the traditional Shannon entropy to estimate the probabilities of possible correspondences being real, the GenICP algorithm (Liu et al. 2006b) employs the generalised Tsallis entropy: $H_T^q = \frac{\sum_j \sum_i m_{ij}^q - 1}{1-q}$ ($q > 0, q \neq 1$) for the same purpose. In this case, the GenICP algorithm describes a more general dynamic:

$$\dot{m_{ij}} = -\beta m_{ij}^q\|\mathbf{p}'_j - \mathbf{R}\mathbf{p}_i - \mathbf{t}\|^2. \quad (4)$$

From the above analysis, it is interesting to note that even though the EvolICP, SoftICP, and GenICP algorithms are apparently different, the dynamics they describe in the iterative process for automatic overlapping range image matching can actually be subsumed into the same more general form:

$$\dot{w_i} = \beta w_i^q (e_i - E), \quad (5)$$

from which we gain a deep insight into the relationship between survival probability and fitness of different individuals and the interaction between different individuals and the environment. Such insight is very valuable to advance overlapping range image matching algorithm development as demonstrated in the next section.

3 The Novel Algorithm

In this section, a novel algorithm is developed based on the replicator equation discussed in the last section for the automatic matching of two overlapping range images that are represented as point clouds: $\mathbf{P}=\{\mathbf{p}_1, \mathbf{p}_2, \ldots, \mathbf{p}_{n_1}\}$ and $\mathbf{P}'=\{\mathbf{p}'_1, \mathbf{p}'_2, \ldots, \mathbf{p}'_{n_2}\}$. The n_1 and n_2 differ mostly since they are different samplings of partially different surface areas. The points from $\mathbf{P}$ and $\mathbf{P}'$ respectively with the same subscript do not mean that they represent correspondences.

To develop the novel algorithm, we make no assumptions about the point clouds to be matched except that the geometry they represent is complex enough for camera motion information delivery and that they have a relatively large (e.g. 60%) overlap in 3D space. These assumptions are reasonable, since it is difficult for any automatic algorithm to deal with sliding errors caused by data with simple (e.g. plane, sphere) geometry. A relatively large overlap between neighbouring views represents typical imaging configurations and can facilitate range image matching. In the process of iterative overlapping range image matching algorithm development, a number of issues often need to be addressed such as establishing possible correspondences, evaluating their probabilities being real, dealing with outliers, minimizing their weighted average matching error, updating camera motion parameters, etc. In this section, the novel algorithm is developed from the following seven aspects: possible correspondence establishment, adaptation of the replicator equation, parameter derivation, fitness estimation, penalty parameter, many-to-one mapping established possible correspondences, and mean field annealing. The final subsection summarizes the novel algorithm.

3.1 Establishment of Possible Correspondences

Given that the camera motion parameters rotation matrix $\mathbf{R}$ and translation vector $\mathbf{t}$ have been initialised or estimated,

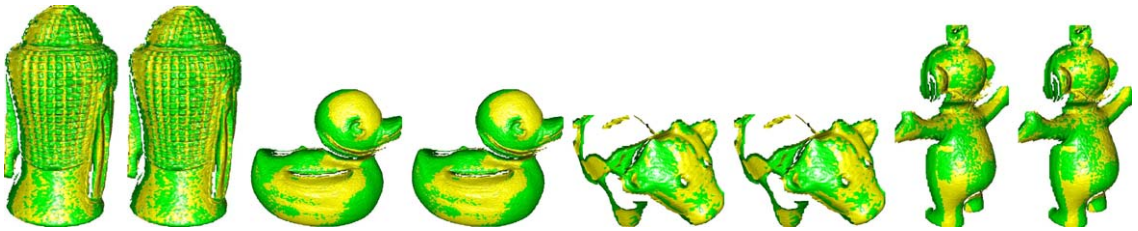

Fig. 2 Matching results of different overlapping range images for the proposed EvolICP algorithm using relative (*odd column*) and absolute (*even column*) fitness differences. *Left two*: buddha140-160; *Second two*: duck160-180; *third two*: cow48-51; *Right two*: tubby180-220

Table 1 The average e_μ and standard deviation e_σ in millimetres of matching errors over RCs, expected and estimated rotation angles θ and $\hat{\theta}$ in degrees of the camera motion, the number N of finally established RCs, and matching time in seconds for the matching of different overlapping range images using the proposed EvolICP algorithm based on relative fitness difference (Reldiff) and absolute fitness difference (Absdiff) respectively

Image	Diff	e_μ (mm)	e_σ (mm)	θ (°)	$\hat{\theta}$ (°)	N	Time (sec.)
buddha140-160	Reldiff	0.60	0.30	20	20.34	10113	73
	Absdiff	0.60	0.30		20.34	10120	111
duck160-180	Reldiff	0.35	0.15	20	19.00	10553	82
	Absdiff	0.35	0.15		19.00	10554	111
cow48-51	Reldiff	0.49	0.39	30	29.90	1892	28
	Absdiff	0.49	0.39		29.87	1892	32
tubby180-220	Reldiff	0.25	0.13	40	40.67	3860	27
	Absdiff	0.26	0.13		40.59	3877	38

for any point $\mathbf{p}_i$ in $\mathbf{P}$, the traditional CPC can be used to determine its possible correspondent $\mathbf{p}'_{c(i)}$ in $\mathbf{P}'$ as:

$$\mathbf{p}'_{c(i)} = \text{argmin}_{\mathbf{p}' \in \mathbf{P}'} \|\mathbf{p}' - \mathbf{R}\mathbf{p}_i - \mathbf{t}\|, \tag{6}$$

where $c(i)$ represents the subscript of a point in $\mathbf{P}'$: $c(i) \in [1, n_2]$. This criterion minimises the *Euclidean* distance between the transformed point $\mathbf{R}\mathbf{p}_i + \mathbf{t}$ and any point $\mathbf{p}'$ in $\mathbf{P}'$. The search space is determined by $\mathbf{P}'$. This criterion is essentially a mapping that associates point $\mathbf{p}'_{c(i)}$ in $\mathbf{P}'$ with a point $\mathbf{p}_i$ in $\mathbf{P}$. The optimised k-D tree data structure (Friedman et al. 1977) was employed to accelerate the closest point search. As a result of this mapping, a set of possible correspondences $(\mathbf{p}_i, \mathbf{p}'_{c(i)})$ has been established between $\mathbf{P}$ and $\mathbf{P}'$. In the following sections, w_i represents the relative frequency, subject to a constraint $\sum_{i=1}^{n_1} w_i = 1$, of a point $\mathbf{p}_i$ in $\mathbf{P}$ being in the overlapping area with $\mathbf{P}'$ and the normalized probability for $\mathbf{p}_i$ in $\mathbf{P}$ to select $\mathbf{p}'_{c(i)}$ in $\mathbf{P}'$ as its possible replicator for estimation of the camera motion parameters, e_i is its fitness whose definition will be discussed below in Sect. 3.4. The relative frequency w_i can be interpreted as the normalized probability of possible correspondence $(\mathbf{p}_i, \mathbf{p}'_{c(i)})$ being real.

3.2 Adaptation of the Replicator Equation

The replicator equation assumes that the relative rate of increase $\dot{w}_i/w_i$ equals the difference between the fitness of an individual and the average fitness $E = \sum_j w_j e_j$ over the entire population. For more computationally efficient and robust range image matching results, we consider the relative fitness difference, rather than the absolute fitness difference, in (1):

$$\dot{w}_i = w_i \frac{e_i - E}{E} \tag{7}$$

so that the effect of the scanning resolutions of range images on the final matching results can be reduced. In this case, the trajectory of evolutionary overlapping range image matching process still lies in the simplex $\mathbf{S}$ defined above, since $\sum_i \dot{w} = 0$ holds.

Some experimental results are presented in Fig. 2 and Table 1, clearly showing that while the replicator equation based on the relative fitness difference produces similar e_μs and e_σs to those based on the absolute fitness difference for the matching of four pairs of overlapping range images, the former reduces the computational time of the latter by a maximum of 34.23% and 25.45% on average. Thus, in the rest of this paper, we will always use the relative fitness

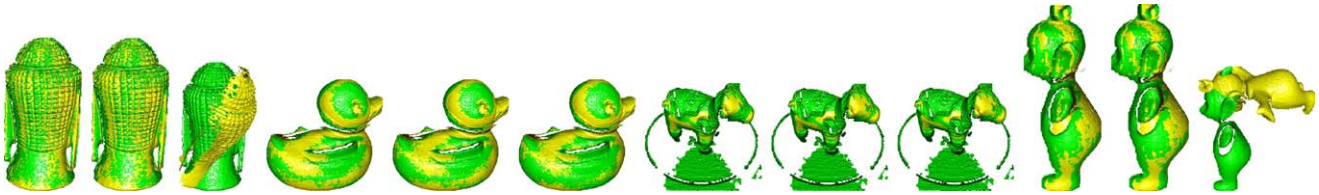

Fig. 3 Matching results of different overlapping range images for the proposed EvolICP algorithm with the fitness of a point defined as functions of the SED between its resulting possible correspondence. *Columns* 1,4,7, and 10: $\tau = 0.0001$; *Columns* 2,5,8, and 11: $\tau = 0.01$; *Columns* 3,6,9 and 12: $\tau = 0.017$. *Left three*: buddha160-180; *Second three*: duck180-200; *Third three*: cow51-54; *Right three*: tubby220-260

difference for efficient automatic overlapping range image matching.

3.3 Parameter Derivation

We would like to apply the replicator equation to model dynamics of the automatic iterative overlapping range image matching process which is actually a discrete one. In this case, we may require the discrete form of the replicator equation which was derived in Alboszta and Miekisz (2004) as: $w_i(t+1) = \frac{w_i(t)e_i(t)}{\sum_j w_j(t)e_j(t)}$. This equation has been applied to successfully find the isomorphism between two graphs in Pelillo (1999). Unfortunately, this equation does not work for overlapping range image matching. This may be because its assumption outlined in the last section was violated. While the existing research usually first discretizes the replicator equations and then applies their discrete form to investigate the problems of interest (Pelillo 1999), we directly use their continuous form to derive the parameters of interest. We rewrite (7) as: $\frac{\dot{w}_i}{w_i} = \frac{e_i - E}{E}$. Integrating both sides of this equation about relative variables w_i on the left hand side and e_i on the right hand side leads to:

$$w_i = \exp((0.5e_i - E)e_i/E). \tag{8}$$

While we are more interested in whether w_i can realistically characterise the probabilities of possible correspondences being real, we temporarily relax the constraint $\sum w_i = 1$ without affecting the camera motion parameter estimation at all in the weighted least squares sense, while $w_i \geq 0$.

3.4 Fitness Estimation

The fitness e_i of an individual $\mathbf{p}_i$ in the current population $\mathbf{P}$ is crucial to determine whether it expands or shrinks in the process of evolution. Thus, it must be carefully defined. In this paper, it is defined as the negative squared Euclidean distance between the possible correspondence $(\mathbf{p}_i, \mathbf{p}'_{c(i)})$: $e_i = -\|\mathbf{p}'_{c(i)} - \mathbf{R}\mathbf{p}_i - \mathbf{t}\|^2$. In this case, the fitness of one individual was estimated independent of that of another. In the real world, however, different individuals in the population usually interact with each other and compete for limited resources in the environment. To simulate the interaction among different individuals and the environment, for the sake of computational efficiency and overlapping range image matching accuracy, the fitness e_i of each individual $\mathbf{p}_i$ in the current population $\mathbf{P}$ is defined as the negative of a power of the squared Euclidean distance (SED) between $(\mathbf{p}_i, \mathbf{p}'_{c(i)})$:

$$e_i = -\|\mathbf{p}'_{c(i)} - \mathbf{R}\mathbf{p}_i - \mathbf{t}\|^{2\tau}, \tag{9}$$

where parameter $\tau \geq 0$ and it denotes the extent to which different individuals in the population interact with each other and the environment.

Some experimental results are presented in Fig. 3 and Table 2, showing that τ must not be too large. For example, when it was set as 0.017, the proposed algorithm failed to match the buddha160-180 and tubby220-260 images, as one intersects the other in 3D space, instead of one being superimposed onto the other. The proposed EvolICP algorithm with $\tau = 0.0001$ produced similar e_μs and e_σs to those with $\tau = 0.01$. The former, however, increases the computational time of the latter by a maximum of 68.11% and 31.46% on average. To achieve a good compromise among stability, accuracy, and computational efficiency, in the rest of this paper, we let $\tau = 0.01$.

3.5 Penalty Parameter

While the fitness of an individual $\mathbf{p}_i$ is defined as the negative of a power of the squared Euclidean distance between $(\mathbf{p}_i, \mathbf{p}'_{c(i)})$, it may be useful for range image matching algorithms to penalise those individuals with low fitness, since the distant points are less likely to be their real replicators. To this end, we introduce a parameter η ($\eta \geq 1$) into (8) as:

$$w_i = \exp((0.5\eta e_i - E)e_i/E) \tag{10}$$

so that these individuals are penalised throughout the whole process of evolution, instead of just at later stages.

Some experimental results on how to determine the penalty parameter η are presented in Fig. 4 and Table 3, showing that η must not be either too large or too small. The proposed algorithm with η taking a value of 5 produced similar e_μs and e_σs to those with η taking a value of 40. However, the latter reduced the computational time of the

Table 2 The average e_μ and standard deviation e_σ of matching errors in millimetres over RCs, expected and estimated rotation angles θ and $\hat{\theta}$ in degrees of the camera motion, the number N of finally established RCs, and matching time in seconds for the matching of different overlapping range images using the proposed EvolICP algorithm with the fitness of a point defined as functions of the SED between its resulting possible correspondence

Image	τ	e_μ (mm)	e_σ (mm)	θ (°)	$\hat{\theta}$ (°)	N	Time (sec.)
buddha160-180	0.0001	0.59	0.24	20	19.96	10982	95
	0.01	0.59	0.25		20.12	10961	66
	0.017	1.25	3.26		81.27	203	187
duck180-200	0.0001	0.31	0.14	20	19.43	12214	116
	0.01	0.31	0.14		19.25	12266	69
	0.017	0.31	0.14		19.27	12223	122
cow51-54	0.0001	0.75	0.40	30	31.25	1096	24
	0.01	0.74	0.41		30.98	1081	23
	0.017	0.73	0.41		30.91	1073	22
tubby220-260	0.0001	0.26	0.14	40	39.22	2494	139
	0.01	0.26	0.14		39.45	2469	127
	0.017	0.74	0.97		89.79	128	164

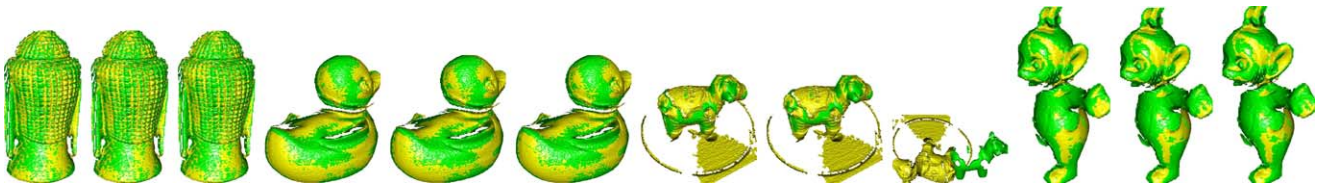

Fig. 4 Matching results of different overlapping range images for the proposed EvolICP algorithm with penalty parameter η taking different values. *Columns* 1,4,7, and 10: $\eta = 5$; *Columns* 2,5,8, and 11: $\eta = 40$; *Columns* 3,6,9, and 12: $\eta = 50$. *Left three*: buddha180-200; *Second three*: duck200-220; *Third three*: cow54-57; *Right three*: tubby260-300

Table 3 The average e_μ and standard deviation e_σ of matching errors in millimetres over RCs, expected and estimated rotation angles θ and $\hat{\theta}$ in degrees of the camera motion, the number N of finally established RCs, and matching time in seconds for the matching of different overlapping range images using the proposed EvolICP algorithm with penalty parameter η taking different values

Image	η	e_μ (mm)	e_σ (mm)	θ (°)	$\hat{\theta}$ (°)	N	Time (sec.)
buddha180-200	5	0.58	0.25	20	19.76	11389	112
	40	0.58	0.26		19.93	11412	81
	50	0.58	0.26		19.90	11410	134
duck200-220	5	0.30	0.13	20	19.42	12087	126
	40	0.30	0.13		19.67	12056	78
	50	0.30	0.13		19.66	12084	149
cow54-57	5	0.68	0.37	30	30.35	2971	1383
	40	0.67	0.36		30.32	2974	1022
	50	3.97	9.25		180.00	32	1032
tubby260-300	5	0.27	0.14	40	39.61	1951	44
	40	0.26	0.14		39.89	1926	39
	50	0.26	0.15		39.91	1925	43

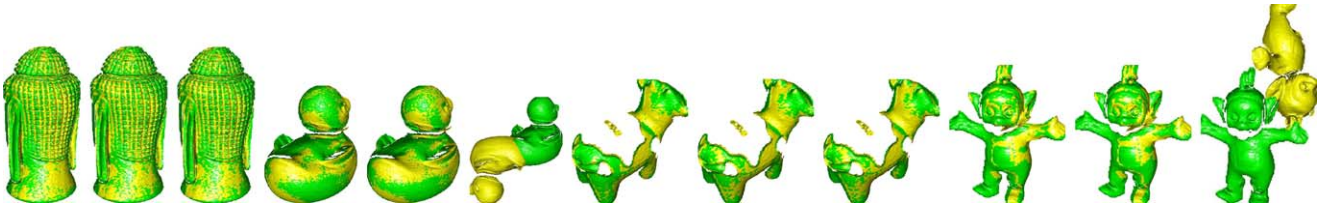

Fig. 5 Matching results of different overlapping range images for the proposed EvolICP algorithm with exponential penalty parameter γ taking different values. *Columns* 1,4,7, and 10: $\gamma = 0.05$; *Columns* 2,5,8, and 11: $\gamma = 2$; *Columns* 3,6,9, and 12: $\gamma = 2.525$. *Left three*: buddha200-220; *Second three*: duck220-240; *Third three*: cow57-60; *Right three*: tubby300-340

Table 4 The average e_μ and standard deviation e_σ of matching errors in millimetres over RCs, expected and estimated rotation angles θ and $\hat{\theta}$ in degrees of the camera motion, the number N of finally established RCs, matching time in seconds for the matching of different overlapping range images using the proposed EvolICP algorithm with exponential penalty parameter γ taking different values

Image	γ	e_μ (mm)	e_σ (mm)	θ (°)	$\hat{\theta}$ (°)	N	Time (sec.)
buddha200-220	0.05	0.59	0.25	20	19.79	11165	68
	2	0.59	0.26		20.05	11117	49
	2.525	0.59	0.26		20.08	11104	78
duck220-240	0.05	0.31	0.15	20	18.94	11314	126
	2	0.30	0.14		19.38	11257	77
	2.525	0.57	0.66		180.00	123	161
cow57-60	0.05	0.49	0.19	30	30.32	3251	26
	2	0.49	0.20		30.58	3246	23
	2.525	0.49	0.20		30.60	3242	26
tubby300-340	0.05	0.25	0.15	40	40.44	2695	28
	2	0.25	0.15		40.65	2689	22
	2.525	0.33	0.25		180.00	146	30

former by a maximum of 38.09% and 25.71% on average. The proposed algorithm with η taking a value of 50 failed to match the cow57-60 images, as the two images have been entirely displaced in 3D space. To exert appropriate penalty and balance accuracy, robustness, and computational efficiency for automatic overlapping range image matching, in the rest of this paper, we let $\eta = 40$.

3.6 Many-to-One Mapping Established Possible Correspondences

While the replicator equation assumes that all the strategies in the population can be chosen by an arbitrary number of players, the range image matching algorithms often assume that a point in one image can only correspond to at most a single point in another and vice versa due simply to the occlusion, appearance and disappearance of points in different range images. The points in $\mathbf{P}$ that choose the same points in $\mathbf{P}'$ as their possible correspondents have to compete for these points (limited resources) as their real correspondents. The resulting correspondences are called many-to-one mapping established possible correspondences (MTOCs). Since MTOCs are unlikely to be simultaneously real, they should be penalised for accurate overlapping range image matching results. To this end, the following three-step scheme is proposed:

- Initialize $w'_j = 1$ $(j = 1, 2, \ldots, n_2)$;
- Accumulate probabilities of MTOCs: $w'_{c(i)} \leftarrow w'_{c(i)} w_i$ $(i = 1, 2, \ldots, n_1)$;
- Re-estimate the probability of each possible correspondence $(\mathbf{p}_i, \mathbf{p}'_{c(i)})$: $w_i \leftarrow (w_i w'_{c(i)})^\gamma$ $(i = 1, 2, \ldots, n_1)$

where a parameter γ ($\gamma > 0$) was introduced to control the extent to which MTOCs were penalized. The rationale behind this penalization scheme is threefold: (1) The relative ranks of different individuals according to their fitnesses are retained; (2) The MTOCs are heavily penalized due to their accumulated probabilities that are usually smaller than 1; and (3) All others are also affected by such MTOCs, since as long as they exist, there is potential for them to compete for limited resources.

Some experimental results are presented in Fig. 5 and Table 4, showing that the exponential penalty parameter γ must not be either too small or too large. The proposed

EvolICP algorithm with γ taking a value of 0.05 produces similar e_μs and e_σs to those with γ taking a value of 2. However, the latter reduces the computational time of the former by a maximum of 38.89% and 24.95% on average. For the matching of the duck220-240 images, the estimated rotation angle of the camera motion has been increased by 2.32%, while the original 18.94° is already quite accurate with respect to the expected 20°. The proposed EvolICP algorithm with γ taking a value of 2.525 failed completely to match the duck220-240 and tubby300-340 images, as it established just hundreds, rather than thousands, of RCs. To exert appropriate penalization and for the sake of robustness, accuracy, and computational efficiency, in the rest of this paper, we let $\gamma = 2$.

3.7 Mean Field Annealing

In order to optimize the probabilities w_i of possible correspondences $(\mathbf{p}_i, \mathbf{p}'_{c(i)})$ being real, we embed them into the powerful deterministic annealing scheme (DAS) (Puzicha et al. 1997):

$$w_i = \exp(\beta(0.5\eta e_i - E)e_i/E), \tag{11}$$

where parameter β ($\beta > 0$) denotes the inverse temperature. The rationale behind this DAS is twofold: (1) It is often powerful enough for a global optimization of the probabilities of possible correspondences established, and (2) It is used to simulate time over which one range image evolves towards another. At the beginning of overlapping range image matching, the camera motion parameters rotation matrix $\mathbf{R}$ and translation vector $\mathbf{t}$ are inaccurate, resulting in the established possible correspondences $(\mathbf{p}_i, \mathbf{p}'_{c(i)})$ being unjustified. This means that all these possible correspondences $(\mathbf{p}_i, \mathbf{p}'_{c(i)})$ are equally likely to be real. Consequently, the inverse temperature β should be small. With the range image matching progressing, the camera motion parameters rotation matrix $\mathbf{R}$ and translation vector $\mathbf{t}$ become more and more accurate, differentiating real correspondences from false ones. In this case, the inverse temperature should be large, penalising those possible correspondences whose fitnesses are significantly lower than the weighted average fitness over the entire population.

3.8 Summary of the Novel EvolICP algorithm

Putting together all the ingredients described in the previous sections, we have the following algorithm for the automatic matching of two overlapping range images represented respectively as point clouds:

Initialize $\mathbf{R}$ to be the identity matrix, $\mathbf{t}$ to be the pure translational motion derived from the centroid difference of the point clouds being matched, starting inverse temperature β_0, inverse temperature $\beta = \beta_0$, inverse temperature increasing rate β_r, final inverse temperature β_f, desired relative variation ρ of camera motion parameters over two successive iterations, maximum iteration number I_0, iteration number $k = 0$, and $w_i^{(k)}$=1/n_1($i = 1, 2, \ldots, n_1$).

Begin A: Do A until $\beta \geq \beta_f$

Begin B: Do B until the relative variation of both rotational and translational vectors at two successive iterations is smaller than ρ or # of iterations $\geq I_0$

Use (6) to establish a set of possible correspondences $(\mathbf{p}_i, \mathbf{p}'_{c(i)})$ between $\mathbf{P}$ and $\mathbf{P}'$ being matched;

Compute the fitness e_i of each individual $\mathbf{p}_i$ in the population $\mathbf{P}$ using (9);

Compute the weighted average fitness over the entire population: $E = \frac{\sum_i w_i^{(k)} e_i}{\sum_i w_i^{(k)}}$;

Update the state variables $w_i^{(k+1)}$ using (11);

Use the procedure described in Sect. 3.6 to penalise the MTOCs;

Begin C: Update camera motion parameters

Use the quaternion method (Besl and McKay 1992) to update camera motion parameters rotation matrix $\mathbf{R}$ and translation vector $\mathbf{t}$ in the weighted least squares sense through optimizing the objective function:

$$J_{3D}(\mathbf{R}, \mathbf{t}) = \min_{\mathbf{R},\mathbf{t}} \sum_{i=1}^{n_1} w_i^{(k+1)} \|\mathbf{p}'_{c(i)} - \mathbf{R}\mathbf{p}_i - \mathbf{t}\|^2;$$

End C

$w_i^{(k)} \leftarrow w_i^{(k+1)}$

$k \leftarrow k + 1$

End B

$\beta \leftarrow \beta_r \beta$;

End A

From the development of the proposed EvolICP algorithm above, it can be seen that it retains the computational complexity, $O(n \ln n)$, of the traditional ICP algorithm accelerated by the k-D tree data structure (Friedman et al. 1977). In the experiments described in this paper, unless otherwise stated, the following parameter values were used: $\beta_0 = 0.00001$, $\beta_r = 1.05$, $\beta_f = 1.0$, $I_0 = 10$, $\rho = 0.001$, $\tau = 0.01$, $\eta = 40$, and $\gamma = 2$.

4 Experimental Results

In this section, we experimentally validate the proposed EvolICP algorithm for automatic matching of overlapping range images depicting objects with various geometrical complexities. For a comparative study of performance, we

duplicated the experimental results of the GA in Silva (2005) and the feature extraction and matching of local surface patches (LSP) (Chen and Bhanu 2007) and implemented the extended version, SoftICP (Liu 2005; Liu 2006), of the SoftAssign algorithm (Gold et al. 1998) and the GenICP algorithm described in Liu et al. (2006b). To deal with main concerns of performance of the proposed EvolICP algorithm, the comparative study is conducted from the following eight aspects: probability evolution, ICP variants for relatively small motions, ICP variants for relatively large motions, image orders, image resolutions, ICP variants and GA, EvolICP and LSP, and overall analysis.

4.1 Probability Evolution

In order to get a rough idea of how the replicator equation evolves the probabilities of possible correspondences established by the traditional CPC being real for the automatic matching of overlapping range images, in this section, we show two examples. One is based on the cow42-39 images and the other on the tubby100-60 images in Fig. 1. For legibility, 10 points were first randomly selected with uniform distribution over all the points in the cow42 and tubby100 images respectively and the evolution of probabilities of their resulting possible correspondences being real is then illustrated. The experimental results are presented in Fig. 6.

Figure 6 shows that at the beginning of matching, all possible correspondences have almost the same probability being real due to inaccurate camera motion parameters. With the matching process progressing, while the probabilities of all these correspondences become smaller and smaller, the relative difference between the minimum and maximum probabilities $w_{\min}$ and $w_{\max}$ of these correspondences be-

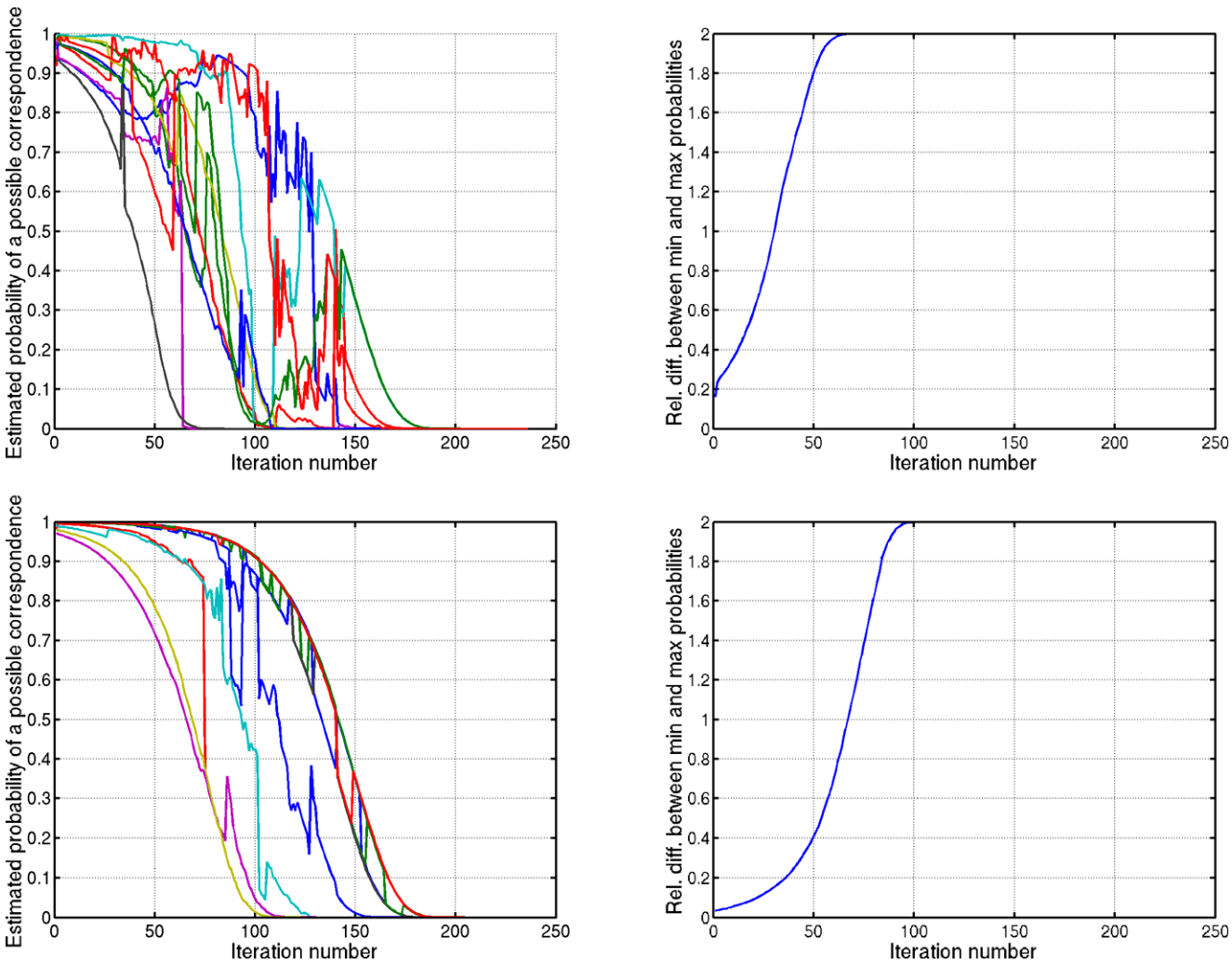

Fig. 6 The evolutionary process of probabilities of possible correspondences established using the traditional CPC being real based on different overlapping range images. *Top row*: cow42-39. *Bottom row*: tubby100-60. *Left column*: the evolutionary process of probabilities of sampled correspondences being real. *Right column*: the relative difference between the minimum and maximum probabilities of all possible correspondences

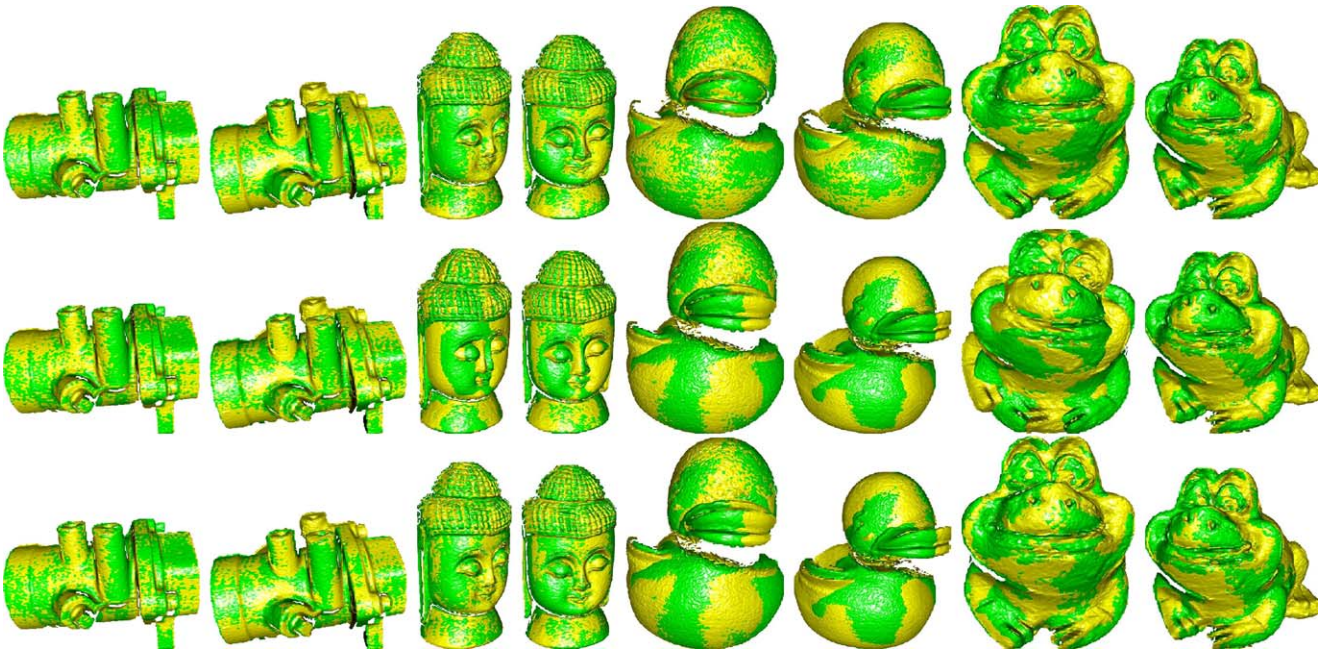

Fig. 7 Matching results of different overlapping range images subject to relatively small motions using different algorithms. From *left column* to *right column*: valve10-0, valve20-10, buddha20-40, buddha0-20, duck120-100, duck140-120, frog20-40, and frog0-20. *Top row*: EvolICP; *Middle row*: SoftICP; *Bottom row*: GenICP

comes larger and larger: $2(w_{\max} - w_{\min})/(w_{\max} + w_{\min})$. After the evolution has terminated, the real correspondences have probabilities larger than zero and false correspondences have probabilities close to zero, resulting in real correspondences being eventually differentiated from false ones. In these two cases, the average registration error e_μ over RCs is 0.67 mm with a scanning resolution of 1.73 mm and the estimated rotation angle of the camera motion is 30.04° with an expectation of 30° for the matching of the cow42-39 images and 0.26 mm with a scanning resolution of 0.84 mm and 39.72° with an expectation of 40° for the matching of the tubby100-60 images. These results clearly show that, despite the fact that the cow42 image is cluttered by the background and has an overlap with the cow39 image as little as $2786/\max(11540, 4774) \times 100\% = 24.14\%$ and the tubby images were captured from side views with an overlap as little as $2041/\max(4713, 4361) \times 100\% = 43.31\%$, the replicator equations have been successfully adapted to model the dynamics in the iterative process for the automatic matching of these images, since the estimated rotation angles of the camera motions are close to the expected ones and the average registration errors are as small as about 1/3 their scanning resolutions. This is a sub-pixel accuracy that a registration algorithm at best can obtain.

4.2 ICP Variants for Relatively Small Motions

In this section, we report the experimental results for the matching of overlapping range images subject to relatively small motions whose rotation angles range between 10° and 20°. Doing so provides ideal conditions for the EvolICP, SoftICP and GenICP algorithms to match overlapping range images. Twelve images were chosen and were three each of a valve, buddha, duck, and frog, as depicted in Fig. 1. The experimental results are presented in Fig. 7 and Table 5.

Figure 7 and Table 5 show that all the three algorithms accurately matched the three valve images with a large amount of interpenetration (Silva 2005) and produced similar e_μs and e_σs. This shows that high quality images are relatively easier to match and different algorithms in this case produce similar matching results. While both the proposed EvolICP and GenICP algorithms estimated a similar rotation angle of the camera motion around 20.00°, the SoftICP algorithm displaced the eyes, noses, and mouths of the buddha in the three buddha images, since it estimated a rotation angle of the camera motion smaller than the expected 20°, increasing the average matching error by as much as 50.00% compared with that produced by the proposed EvolICP algorithm. This shows that the traditional Shannon entropy is less competent for describing the dynamics of iterative automatic overlapping range image matching process. While the proposed EvolICP algorithm produced a relative error of 2.45% in the estimation of the rotation angle of the camera motion for the matching of the duck140, duck120, and duck100 images, the SoftICP and GenICP algorithms produced the same parameter as much as 70.90% and 7.40% respectively. The inaccurate matching results have been illustrated as sepa-

Table 5 The average e_μ and standard deviation e_σ of matching errors in millimetres over RCs, expected and estimated rotation angles θ and $\hat{\theta}$ in degrees of the camera motion, the number N of finally established RCs, and matching time in seconds for different algorithms applied to different overlapping range images subject to relatively small motions

Image	Algo.	e_μ (mm)	e_σ (mm)	θ (°)	$\hat{\theta}$ (°)	N	Time (sec.)
valve10-0	EvolICP	0.38	0.20	10	10.12	11024	34
	SoftICP	0.38	0.21		10.11	11028	39
	GenICP	0.38	0.21		10.11	11056	32
valve20-10	EvolICP	0.40	0.23	10	10.13	10827	153
	SoftICP	0.40	0.22		10.10	10856	59
	GenICP	0.40	0.23		10.11	10867	67
buddha20-40	EvolICP	0.58	0.25	20	20.22	10753	136
	SoftICP	0.87	0.53		8.49	8825	68
	GenICP	0.58	0.25		20.01	10784	124
buddha0-20	EvolICP	0.58	0.25	20	20.38	10997	109
	SoftICP	0.72	0.35		17.67	10251	45
	GenICP	0.58	0.24		20.05	11022	141
duck120-100	EvolICP	0.26	0.11	20	19.51	7541	75
	SoftICP	0.36	0.23		11.55	7137	45
	GenICP	0.27	0.13		18.52	7522	66
duck140-120	EvolICP	0.29	0.13	20	19.91	8372	136
	SoftICP	0.47	0.32		5.82	7107	41
	GenICP	0.30	0.14		18.89	8423	88
frog20-40	EvolICP	0.29	0.30	20	19.18	5574	156
	SoftICP	0.42	0.36		16.50	3112	37
	GenICP	0.29	0.30		19.13	5559	57
frog0-20	EvolICP	0.30	0.15	20	18.96	5799	98
	SoftICP	0.32	0.17		17.82	5667	52
	GenICP	0.30	0.15		19.10	5776	51

rating the left wings of the duck in the three duck images with less interpenetration. This shows that the generalized Tsallis entropy is less powerful in characterising the dynamics of iterative automatic overlapping range image matching process. While both the proposed EvolICP and GenICP algorithms aligned the three frog images very well with an average matching error over RCs being around 0.29 mm, the SoftICP algorithm increased their average matching error by as much as 44.83%, as confirmed by the fact that the frogs in the transformed frog20 and frog40 images intersect in 3D space. These results show that the adapted replicator equation in conjunction with the deterministic annealing scheme is powerful in estimating and optimizing the probabilities of possible correspondences for automatic overlapping range image matching, producing accurate and stable results, even though the prior knowledge about occlusion, appearance and disappearance of points in different range images was not available at all.

4.3 ICP Variants for Relatively Large Motions

Large motions are of practical importance, since they can reduce the overhead of image acquisition and also resulting image processing. Thus, in this section, we carry out experiments using overlapping range images subject to relatively large motions with rotation angles as large as 40° in 3D space. Such images however are more challenging to match, since they usually include a large number of appearing and disappearing points, which lead the CPC to establish a large number of false correspondences, rendering it harder for any ICP variant to differentiate feasible correspondences from false ones. Due to the fact that large motions violate the assumption of the traditional ICP algorithm that requires a good initialization of the camera motion parameters, it is expected that all the ICP variants will generally produce poor matching results. However, our interest is in testing how the proposed EvolICP algorithm actually behaves in matching overlapping range images subject to relatively large mo-

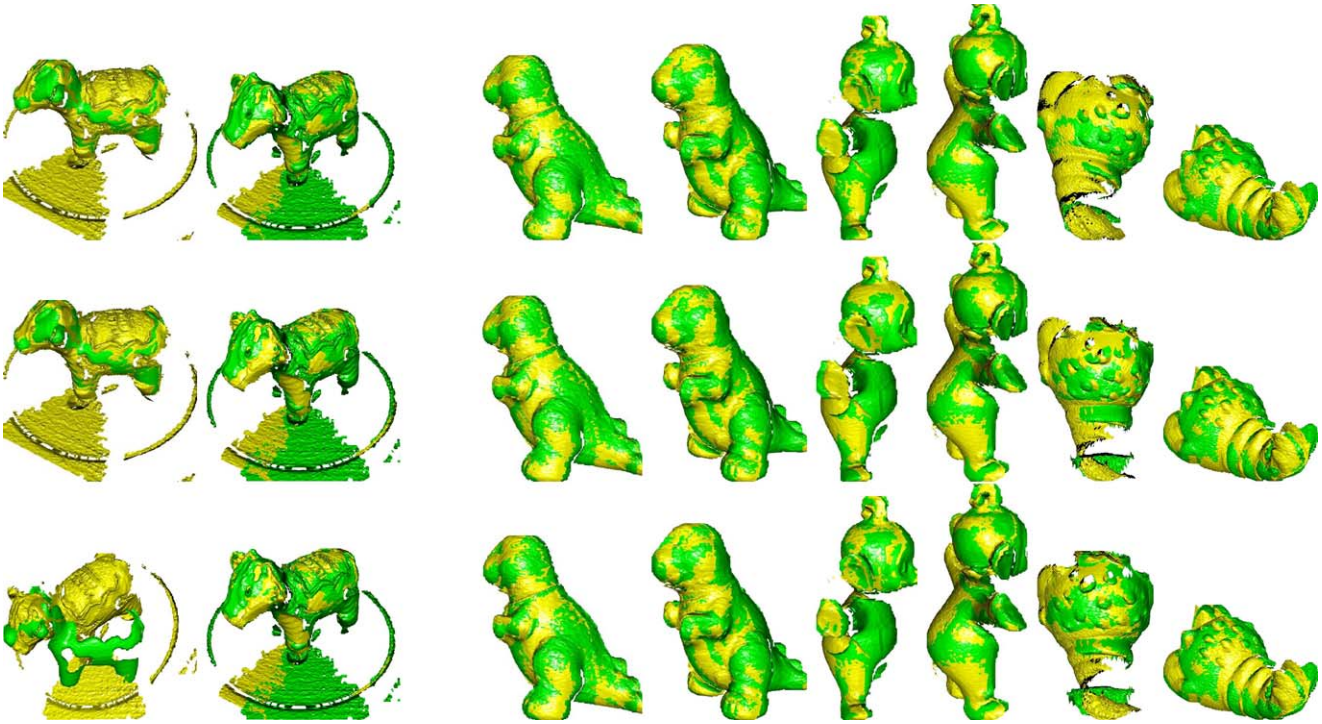

Fig. 8 Matching results of different overlapping range images subject to relatively large motions using different algorithms. From *left column* to *right column*: cow42-39, cow45-42, dinosaur36-0, dinosaur72-36, tubby100-60, tubby140-100, lobster100-60, and lobster140-100. *Top row*: EvolICP; *Middle row*: SoftICP; *Bottom row*: GenICP

tions. For this purpose, twelve real images were selected of a cow, dinosaur, tubby, and lobster, as depicted in Fig. 1. The experimental results are presented in Fig. 8 and Table 6.

From Fig. 8 and Table 6, it can be seen that even though the cow42 image is cluttered, the proposed EvolICP algorithm still accurately matched the cow42-39 images. In contrast, the GenICP algorithm failed to match them, since the transformed cow42 image intersects the cow39 image in 3D space. All of the EvolICP, SoftICP, and GenICP algorithms accurately matched the high quality dinosaur images. While all the three algorithms estimated for the matching of the tubby140-100 images the rotation angle of the camera motion close to the expected 40°, the SoftICP algorithm converged pre-maturely for the matching of the tubby100-60 images and estimated a rotation angle of the camera motion smaller than 36°, increasing the average matching error by as much as 23.08% compared with that produced by the proposed EvolICP algorithm. The inaccurate matching of the SoftICP algorithm has been manifested as clearly separating the hands of the tubby in the transformed tubby100 and tubby60 images. While the GenICP algorithm produced a relative error of 7.07% in the estimation of the rotation angle of the camera motion for the matching of the lobster100-60 images, all the three algorithms produced a similar average matching error around 0.43 mm for the matching of the lobster140-100 images. These results show that, even though it was still initialized by the pure translational motion derived from the centroid difference of the images being matched that were subject to relatively large motions with rotation angles as large as 40° in 3D space, the proposed EvolICP algorithm still successfully evolved the first range images towards the target ones, yielding accurate and stable results.

4.4 Image Orders

Since only the closest points in the second image were used for matching, a concern as to whether the order of images (from image A to image B or from image B to image A) affects the proposed EvolICP algorithm on the final matching results arises. To deal with this concern, we carried out experiments in this section while reversing the order of images. The experimental results are presented in Fig. 9 and Table 7.

Figure 9 and Table 7 show that all the three algorithms exhibit similar behaviour in matching both the buddha and duck images to that in matching the original images. They all accurately matched the cow39-42 images with the estimated rotation angle of the camera motion close to the expected 30°. The GenICP algorithm produced a relative variation of 14.42% in the estimated rotation angle of the camera motion for the matching of the cow42-39 and cow39-42 images. While the proposed EvolICP algorithm still

Table 6 The average e_μ and standard deviation e_σ of matching errors in millimetres over RCs, expected and estimated rotation angles θ and $\hat{\theta}$ in degrees of the camera motion, the number N of finally established RCs, and matching time in seconds for different algorithms applied to different overlapping range images subject to relatively large motions

Image	Algo.	e_μ (mm)	e_σ (mm)	θ (°)	$\hat{\theta}$ (°)	N	Time (sec.)
cow42-39	EvolICP	0.67	0.99	30	30.04	2786	999
	SoftICP	0.72	0.41		29.83	2784	165
	GenICP	1.03	1.08		26.05	572	382
cow45-42	EvolICP	0.75	0.47	30	30.18	3026	35
	SoftICP	0.87	0.59		27.38	2840	25
	GenICP	0.80	0.51		28.54	2958	37
dinosaur36-0	EvolICP	0.57	1.19	36	35.80	5189	137
	SoftICP	0.57	1.19		35.66	5214	45
	GenICP	0.57	1.19		35.73	5214	53
dinosaur72-36	EvolICP	0.60	0.37	36	35.20	3790	61
	SoftICP	0.60	0.36		35.11	3778	29
	GenICP	0.60	0.36		35.12	3799	37
tubby100-60	EvolICP	0.26	0.19	40	39.72	2041	116
	SoftICP	0.32	0.23		35.66	2052	24
	GenICP	0.26	0.19		39.60	2059	48
tubby140-100	EvolICP	0.27	0.13	40	39.53	3015	55
	SoftICP	0.27	0.17		39.55	3005	28
	GenICP	0.27	0.13		39.61	2994	33
lobster100-60	EvolICP	0.45	0.31	40	39.36	3129	127
	SoftICP	0.47	0.37		40.04	2754	44
	GenICP	0.43	0.34		37.17	3172	106
lobster140-100	EvolICP	0.44	0.26	40	38.51	6180	65
	SoftICP	0.42	0.23		38.85	6123	42
	GenICP	0.43	0.24		38.55	6103	65

produced accurate matching results, both the SoftICP and GenICP algorithms misplaced the necks and tails of the lobster in the transformed lobster60 and lobster100 images, yielding a relative variation as much as 42.02% in the average matching error of RCs and as much as 39.84% in the estimated rotation angle of the camera motion before and after reversing the image orders. These results show that image orders do impose a subtle effect on the final matching results of the ICP variants.

4.5 Image Resolutions

Image resolution imposes a remarkable effect on the final matching results. Denser sampling in the process of scanning is often useful to capture more accurately the geometry of the objects of interest. Different scanning processes usually do not produce exactly the same sampled data. The denser the sampling, the less the difference between the sampled data, and thus the more likely the established real correspondences represent exactly the same points on the surface of the objects of interest. However, the error in the assumption regarding pointwise correspondence never truly goes away. This is a limitation of all the matching approaches based on sampled data. In this section, we carry out experiments with the data acquired using another scanner, MSU's Technical Arts 100X. The images include not only isolated objects, as is the case for the range images captured using the Minolta Vivid 700 range camera, but also two objects occluding each other. The resolutions of these images vary from 77×114 (adapter-3) to 240×240 (occl4 and occl5). The experiments based on such images can reveal whether the proposed EvolICP algorithm is sensitive to different sampling densities, noise characteristics, etc. Due to the fact that the images include a large number of points (23353 in bigwye-3), for the sake of computational efficiency, the inverse temperature increasing rate was reset as $\beta_r = 1.1$. The experimental results are presented in Fig. 10 and Table 8.

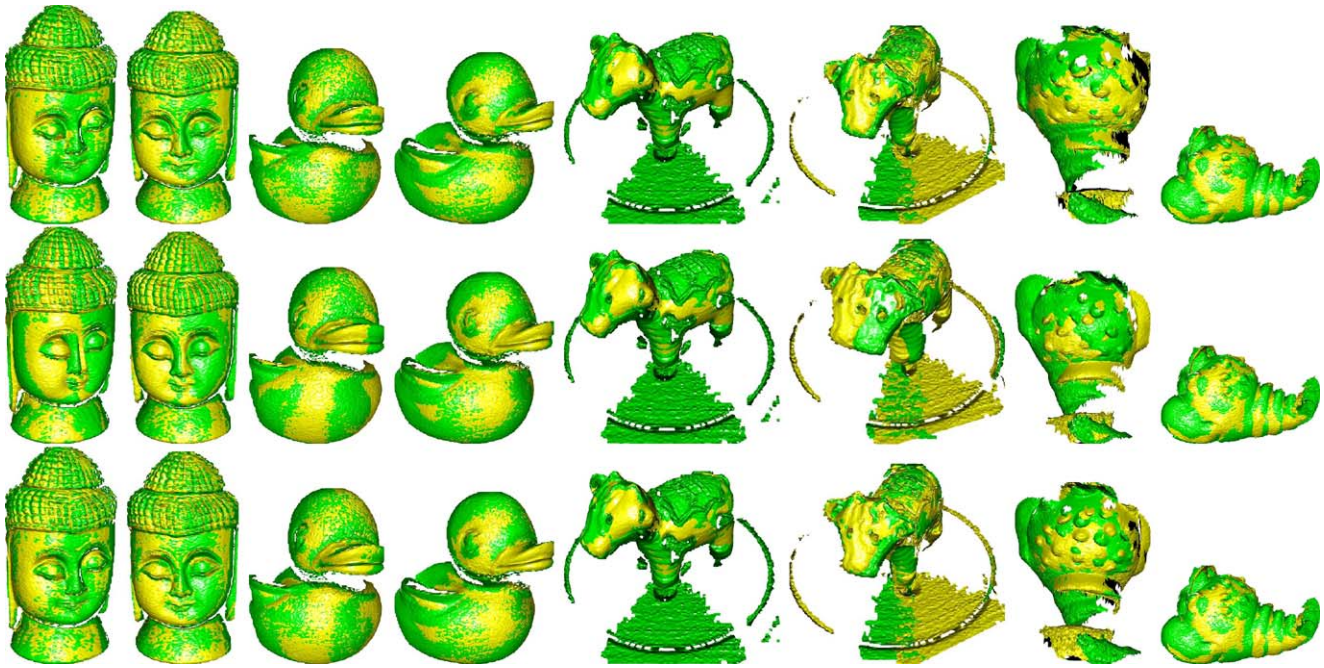

Fig. 9 Matching results of different algorithms based on different overlapping range images with reversed orders. From *left column* to *right column*: buddha40-20, buddha20-0, duck100-120, duck120-140, cow39-42, cow42-45, lobster60-100, and lobster100-140. *Top row*: EvolICP; *Middle row*: SoftICP; *Bottom row*: GenICP

Figure 10 and Table 8 show that, while all the three algorithms accurately matched the high quality adapter2-3 images, they all failed to match the agpart2-1 images. It is interesting to note that, while the transformed agpart2 and agpart1 images aligned by either the SoftICP or GenICP algorithm intersect in 3D space, the proposed EvolICP algorithm maximized the overlapping area between the two perpendicular cylinders in the two images, yielding decent matching results. While the SoftICP algorithm failed to match the curvblock2 and adapter+curvblock images, both the proposed EvolICP and GenICP algorithms managed to correctly align them, despite the fact that the curvblock in the adapter+curvblock image was occluded by an adapter. Even though all the three algorithms estimated the rotation angle of the camera motion around 40° for the matching of the hump3-1 images, the SoftICP algorithm produced an average matching error 25.15% larger than that produced by either the proposed EvolICP or GenICP algorithm. While both the proposed EvolICP and SoftICP algorithms produced similar results for the matching of the block12-1 images, the GenICP algorithm increases the average matching error by as much as 197.81% compared with that produced by the proposed EvolICP algorithm. The occl4-5 images are even more challenging to match, since they include only a small cylinder in the overlapping area. Even so, the proposed EvolICP algorithm still succeeded in matching. Both the SoftICP and GenICP algorithms displaced the two cylinders in the occl4 and occl5 images, increasing the average matching error by up to 201.92% compared with that of the proposed EvolICP algorithm. All the three algorithms produce similar average errors for the matching of the cap2-3 images. The reason why their estimated rotation angles of the camera motion are quite different is that the cap in the two images includes relatively simple geometry and thus, sliding matching error occurred. While both the proposed EvolICP and GenICP algorithms produced similar results for the matching of the bigwye3-4 images, the SoftICP algorithm increased the average matching error by as much as 18.29% compared with that produced by either the proposed EvolICP or GenICP algorithm. These results show that the variation of scanning resolution, noise characteristics, etc. does not really impose a significant effect on the proposed EvolICP algorithm for accurate and robust overlapping range image matching results.

4.6 ICP Variants and GA

While the ICP variants firstly search possible correspondences in the image space and then update the camera motion parameters, we compare them in this section to the latest genetic algorithm (GA) (Silva 2005) that takes an opposite strategy for overlapping range image matching. Due to lack of details, we did not implement the original GA. Instead, we duplicated part of Table 2 with respect to the comparative MSE and SIM results in the original paper. The definitions of MSE (mean square error) and SIM (surface interpenetration measure) can be found in Silva (2005). To show the

Table 7 The average e_μ and standard deviation e_σ of matching errors in millimetres over RCs, expected and estimated rotation angles θ and $\hat{\theta}$ in degrees of the camera motion, the number N of finally established RCs, and matching time in seconds for different algorithms applied to different overlapping range images with reversed orders

Image	Algo.	e_μ (mm)	e_σ (mm)	θ (°)	$\hat{\theta}$ (°)	N	Time (sec.)
buddha40-20	EvolICP	0.58	0.24	20	20.15	10583	94
	SoftICP	0.82	0.48		11.92	9050	47
	GenICP	0.58	0.25		19.95	10566	117
buddha20-0	EvolICP	0.58	0.25	20	20.39	10732	66
	SoftICP	0.71	0.35		17.69	9986	40
	GenICP	0.58	0.24		20.13	10756	164
duck100-120	EvolICP	0.26	0.13	20	19.25	6952	53
	SoftICP	0.33	0.19		13.90	6673	27
	GenICP	0.28	0.13		17.95	6940	59
duck120-140	EvolICP	0.29	0.14	20	19.98	6987	50
	SoftICP	0.33	0.17		17.34	6868	31
	GenICP	0.31	0.15		18.78	7014	60
cow39-42	EvolICP	0.73	0.41	30	29.74	1822	24
	SoftICP	0.73	0.41		29.94	1800	19
	GenICP	0.73	0.42		30.10	1781	22
cow42-45	EvolICP	0.72	0.52	30	30.07	3794	322
	SoftICP	0.84	0.81		19.04	3046	73
	GenICP	0.74	0.46		28.97	3847	120
lobster60-100	EvolICP	0.43	0.30	40	38.90	2913	250
	SoftICP	0.72	0.67		59.96	2159	50
	GenICP	0.54	0.40		31.52	2422	97
lobster100-140	EvolICP	0.42	0.23	40	38.84	5389	61
	SoftICP	0.44	0.27		38.37	5499	42
	GenICP	0.44	0.27		38.17	5485	53

implementation difference, we also implemented Zhang's ICP algorithm (Zhang 1992). The experimental results are presented in Table 9, in which the proposed EvolICP and Zhang's ICP algorithms were implemented in this paper, while the ICP3 and GA algorithms were implemented in Silva (2005). While Zhang's ICP algorithm classifies all possible correspondences into either real or false ones, the proposed EvolICP algorithm uniformly estimates their probabilities being real. Thus, while the MSE for the former is computed over real correspondences, the same parameter for the latter is computed over RCs.

From Table 9, it can be seen that the implementation, ICP3, of Zhang's ICP algorithm in Silva (2005) differs from ours, as they did not produce the same matching results in the sense of either MSE or SIM, even though the same images were used for the experiments. This may be because they used different methods to estimate surface normals required either for the orientation consistency test in the algorithm or for the calculation of SIM in this paper. While 7 SIMs out of 10 from our implementation of Zhang's ICP algorithm are smaller than those in Silva (2005), 9 SIMs out of 10 from the novel EvolICP algorithm are smaller than those of the GA (Silva 2005). As admitted in Silva (2005), SIM is most effective at refining good alignments to achieve precise alignments. For instance, a "correct" alignment with low MSE may exhibit no interpenetration if the aligned surfaces are parallel but slightly displaced. The proposed EvolICP algorithm always produces the smallest MSE and thus, in this case is the best, compared with the ICP3 and GA algorithms for the matching of the 15 range images selected. These 15 images were chosen by Ref. (Silva 2005). The reason why we also selected them for the experiments was to compare the proposed EvolICP algorithm against the GA based on the same data. It is also noted that the classification based Zhang's ICP algorithm is not stable. While it accurately matched the tubby images, it inaccurately matched the bird and frog images. This also explains why we did not choose the classification based ICP variants (Liu et al. 2000, 2006a; Pulli 1999; Turk and Levoy 1994; Liu and Wei 2004) for a comparative study in this paper.

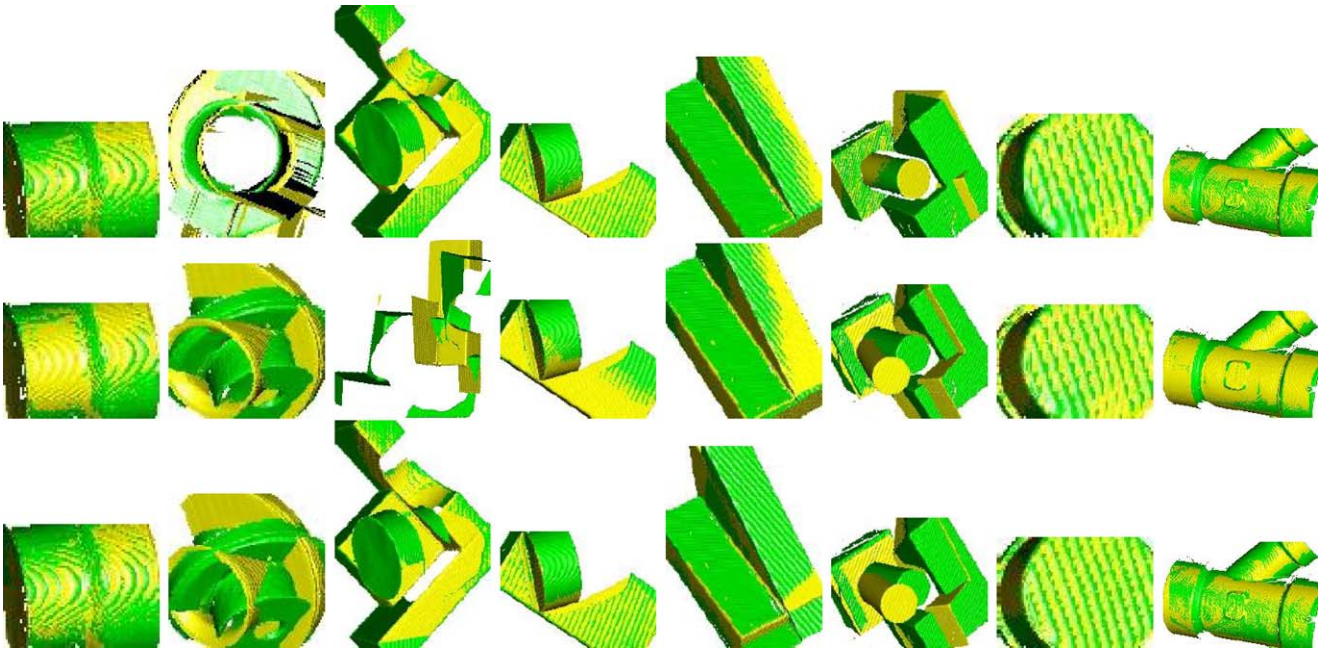

Fig. 10 Matching results of different algorithms based on different overlapping range images with various resolutions. From *left column* to *right column*: adapter2-3, agpart2-1, curvblock2-adapter+curvblock, hump3-1, block12-1, occl4-5, cap2-3, and bigwye3-4. *Top row*: EvolICP; *Middle row*: SoftICP; *Bottom row*: GenICP

4.7 EvolICP and LSP

The proposed EvolICP algorithm evolves the probabilities of possible correspondences established using the traditional CPC. In this section, we compare it against a latest algorithm (Chen and Bhanu 2007) that extracts and matches features of local surface patches (LSP) based on the same data. Due to limited time, we did not implement the original LSP algorithm. Instead, we duplicated part of Table 4 with respect to verification results for single-object scenes in the original paper. The experimental results are presented in Table 10.

Table 10 shows that for the registration of 20 pairs of overlapping range images, the proposed EvolICP algorithm increased in the worst two cases the registration error slightly by 17.86% for the registration of the cow71-73 images and by 6.57% for the registration of the pat-2img108-144 images. In the best two cases, however, it decreased the registration error remarkably by as much as 39.98% for the registration of the brain144-180 images and by as much as 32.97% for the registration of the frog2-220-240 images. These results show that the proposed EvolICP algorithm is powerful in registering various range images with different complexities of geometries through an effective modelling of the dynamics in the iterative process of registration.

To elaborate the performance of the proposed EvolICP algorithm, we estimated the overlap between the cow71-73 images to be $3155/\max(11575, 5005) \times 100\% = 26.91\%$ and the rotation angle of their camera motion to be 19.82°, the overlap between the pat-2img108-144 images to be $9879/\max(14773, 15941) \times 100\% = 61.97\%$ and the rotation angle of their camera motion to be 17.58° with an expectation of 20°. The final registration results of these two pairs of images are presented in Fig. 11, clearly showing that the images have not been registered as poorly as either the registration error or the rotation angle of the camera motion indicated.

These results show that despite the fact that the LSP algorithm extracts and matches features of points of interest, producing a coarse estimate of the camera motion parameters, which are then refined by a classification based ICP variant (Zhang 1992), the final registration results in the sense of root mean square (RMS) registration error are not always more accurate than those produced by the proposed EvolICP algorithm initialized using just the pure translational motion derived from the centroid difference of overlapping range images being registered. This is because the estimation of either the shape index or surface orientation in the LSP method is sensitive to imaging noise, low image resolution, occlusion, appearance and disappearance of points, it is difficult for the LSP features to represent the simple and repetitive geometry in the brain and frog2 images, for example. Due to data dependence, it is also difficult for the classification based ICP variant (Zhang 1992) to set up relative thresholds for the rejection of false matches, yielding poor registration results. This observation is consistent with the experimental results reported in the last section on the comparative study of ICP variants and GA.

Table 8 The average e_μ and standard deviation e_σ of matching errors in millimetres over RCs, estimated rotation angle $\hat{\theta}$ in degrees of the camera motion, the number N of finally established RCs, and matching time in seconds for different algorithms applied to different overlapping range images with various resolutions

Image	Algo.	e_μ (mm)	e_σ (mm)	$\hat{\theta}$ (°)	N	Time (sec.)
adapter2-3	EvolICP	0.0162	0.0074	19.75	4087	11
	SoftICP	0.0165	0.0070	19.03	4064	7
	GenICP	0.0162	0.0072	19.17	4057	13
agpart2-1	EvolICP	0.0205	0.0171	89.27	2145	222
	SoftICP	0.0349	0.0412	37.94	435	59
	GenICP	0.0322	0.0305	30.51	460	134
curvblock2-adapter+curvblock	EvolICP	0.0175	0.0077	25.98	6615	529
	SoftICP	0.0415	0.0430	8.11	816	207
	GenICP	0.0173	0.0071	25.94	6574	264
hump3-1	EvolICP	0.0159	0.0063	40.45	6355	210
	SoftICP	0.0199	0.0072	39.51	6253	91
	GenICP	0.0159	0.0061	40.53	6384	132
block12-1	EvolICP	0.0183	0.0068	51.44	5761	126
	SoftICP	0.0209	0.0079	51.10	5788	99
	GenICP	0.0545	0.0642	44.97	3772	273
occul4-5	EvolICP	0.0208	0.0500	10.69	5172	844
	SoftICP	0.0628	0.0837	11.99	1525	159
	GenICP	0.0551	0.0654	7.14	1761	689
cap2-3	EvolICP	0.0152	0.0067	46.10	4004	9
	SoftICP	0.0154	0.0069	44.64	3992	9
	GenICP	0.0150	0.0059	26.75	4246	13
bigwye3-4	EvolICP	0.0164	0.0065	42.69	15669	515
	SoftICP	0.0194	0.0078	42.68	15579	270
	GenICP	0.0167	0.0067	42.71	15627	401

Table 9 The mean square error (MSE) in squared millimetres and surface interpenetration measure (SIM) in percentage of different algorithms applied to different overlapping range images

Image	EvolICP		Zhang		ICP3		GA	
pair	MSE (mm^2)	SIM (%)	MSE (mm^2)	SIM (%)	MSE (mm^2)	SIM (%)	MSE (mm^2)	SIM (%)
bird0-20	0.0976	53.2	2.6030	52.6	0.3950	64.6	0.4299	90.7
bird20-40	0.0943	53.0	1.6696	49.3	1.2689	53.8	1.4440	91.3
duck0-20	0.2119	38.9	0.4503	39.1	0.7002	39.9	0.8017	57.0
duck20-40	0.2049	39.8	3.0000	51.0	0.8968	38.7	0.9841	56.3
frog0-20	0.1165	60.6	3.5063	68.2	0.3468	74.5	0.3615	82.7
ww frog20-40	0.1749	41.9	1.5649	44.5	0.8300	69.5	0.8180	80.8
lobster0-20	0.1941	60.0	0.6041	60.1	0.9949	38.1	1.2573	60.9
lobster20-40	0.2135	61.2	1.8362	61.4	3.1948	28.8	3.9504	55.9
tubby0-20	0.0695	60.3	0.1923	60.4	0.2270	80.9	0.2393	91.0
tubby20-40	0.0714	59.0	0.2730	59.7	0.4334	80.2	0.4495	90.3

Table 10 The root mean square (RMS) registration error in millimetres of different algorithms applied to different overlapping range images

Image	Algo.	RMS (mm)	Image	Algo.	RMS (mm)
angel20-40	EvolICP	0.537	lobster0-20	EvolICP	0.373
	LSP	0.624		LSP	0.525
bunny40-60	EvolICP	0.212	tubby340-0	EvolICP	0.245
	LSP	0.217		LSP	0.252
frog240-260	EvolICP	0.280	brain144-180	EvolICP	0.548
	LSP	0.263		LSP	0.913
peach240-260	EvolICP	0.248	duck0-20	EvolICP	0.379
	LSP	0.236		LSP	0.426
bird300-320	EvolICP	0.286	orange-dino0102-0104	EvolICP	0.456
	LSP	0.314		LSP	0.481
cow71-73	EvolICP	0.6638	valve0-20	EvolICP	0.405
	LSP	0.5632		LSP	0.395
frog2-220-240	EvolICP	0.250	buddha20-40	EvolICP	0.584
	LSP	0.373		LSP	0.632
pooh180-200	EvolICP	0.283	frame015-017	EvolICP	0.416
	LSP	0.306		LSP	0.459
blue-dino0125-0375	EvolICP	0.491	pat-2img108-144	EvolICP	0.779
	LSP	0.504		LSP	0.731
dough-boy20-0	EvolICP	0.215	yellowhorn252-288	EvolICP	0.508
	LSP	0.214		LSP	0.732

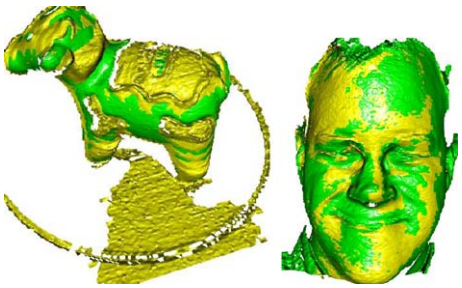

Fig. 11 Matching results of the cow71-73 (*left*) and pat-2img108-144 (*right*) images using the proposed EvolICP algorithm

4.8 Overall Analysis

The statistics of the experimental results reported above in this section are presented in Table 11. From Table 11, it can be seen that: (1) while both SoftICP and GenICP algorithms sometimes produced misalignments, the EvolICP algorithm usually produces relatively stable alignments. This conclusion has been verified by the fact that the GenICP algorithm completely failed to match the cow42-39 images. While the SoftICP algorithm failed to match the agpart2-1, curvblock2-adapter+curvblock, and occl4-5 images, the GenICP algorithm failed to match the agpart2-1 and occl4-5 images. The resolutions, noise characteristics, etc. do not really impose a significant impact on the behaviour of the proposed EvolICP algorithm in the sense of robustness for automatic overlapping range image matching; and (2) The proposed EvolICP algorithm produced the most accurate and stable matching results in the sense of average and standard deviation of matching errors of RCs, but is the most time consuming, for the automatic matching of overlapping range images captured using either the Minolta Vivid 700 or Technical Arts 100X range scanner. For the range images captured using the Minolta Vivid 700 range scanner, even though the SoftICP algorithm requires just about 30% of the time required by the proposed EvolICP algorithm for matching and is thus the most computationally efficient, it produced the worst matching results, increasing the average matching error by as much as 17.39% compared with that produced by the proposed EvolICP algorithm. For the range images captured using the Technical Arts 100X range scanner, the proposed EvolICP algorithm reduces the average matching error by as much as 39.10% compared with that produced by the SoftICP algorithm and by as much as 36.92% compared with that produced by the GenICP algorithm. The proposed EvolICP algorithm produced smaller MSE over RCs, and also smaller SIM than the GA.

Compared with the LSP method, the proposed EvolICP algorithm decreased its registration error by as much as

Table 11 The average μ and standard deviation σ of average matching errors e_μ and standard deviations e_σ in millimetres, and matching time in seconds, MSE in squared millimetres, SIM in percentage, and RMS in millimetres of different algorithms based on range images captured using different scanners

Scanner	Measure	Method	e_μ (mm)	e_σ (mm)	Time (sec.)
Minolta		EvolICP	0.46	0.32	142.17
	μ	SoftICP	0.54	0.39	46.54
		GenICP	0.49	0.33	86.62
		EvolICP	0.16	0.25	190.99
	σ	SoftICP	0.20	0.26	27.89
		GenICP	0.20	0.26	71.80
Technical Arts		EvolICP	0.0176	0.0136	308.25
	μ	SoftICP	0.0289	0.0255	112.62
		GenICP	0.0279	0.0256	239.87
		EvolICP	0.0020	0.0142	275.39
	σ	SoftICP	0.0155	0.0264	87.50
		GenICP	0.0161	0.0247	210.70
		MSE (mm^2)	SIM (%)		
Minolta		EvolICP	0.14	52.79	
	μ	ICP3	0.93	56.90	
		GA	1.07	75.69	
		EvolICP	0.06	8.71	
	σ	ICP3	0.82	18.49	
		GA	1.03	15.26	
		RMS (mm)			
Minolta	μ	EvolICP	0.4122		
		LSP	0.4580		
	σ	EvolICP	0.1619		
		LSP	0.1968		

10.00% and registered 15 pairs out of 20 of overlapping range images more accurately. Note that such improvement is obtained after the LSP registration results have already been refined by a classification based ICP variant (Zhang 1992). Thus, it can be concluded that the LSP algorithm does not always provide good enough coarse initial camera motion parameters for the ICP variant (Zhang 1992) to refine. This conclusion has been demonstrated by the fact that the bird300 image is best matched by the LSP method with a frog2-220 image and both the pat-2img108 and pooh180 images with the duck0 image. These results show that it is challenging for the LSP method to define expressive features for the representation of the points of interest and it has inherent ambiguity in determining real point matches (Makadia et al. 2006). The pure translational motion is usually a good choice for the initialization of the camera motion parameters for the EvolICP algorithm to evolve possible correspondences, leading to accurate registration results, especially for the registration of overlapping range images subject to various camera motions with rotation angles smaller than 40°, for example.

5 Discussion and Conclusions

5.1 Discussion

Through the experiments based on real range images presented in this paper, we have made the following observations:

Range image matching theory will become much more useful if we can efficiently handle its mathematical models. For example, assuming that we adopt a dynamic model for the strategic evolution of one range image towards another, how efficiently (if ever) can we answer the model's long term behaviour? Can we predict that an evolutionary range image matching process will stabilize, say, to an evolutionarily stable strategy (ESS): $\|\mathbf{p}'_{c(i)} - \mathbf{R}\mathbf{p}_i - \mathbf{t}\| \leq \|\mathbf{p}'_{c(i)} - (\mathbf{R} + \delta\mathbf{R})\mathbf{p}_i - (\mathbf{t} + \delta\mathbf{t})\|$ where $\delta\mathbf{R}$ and $\delta\mathbf{t}$ are small

perturbations of the camera motion parameters rotation matrix and translation vector respectively? Even more, given the range images that algorithms match and given the description of the adaptation and learning forces, can we claim that such an evolutionary range image matching process will indeed have an ESS? Can we compute how this ESS will look like, in the case of an affirmative answer? Can we claim that the established point matches $(\mathbf{p}_i, \mathbf{p}'_{c(i)})$ between two overlapping range images correspond to the Nash equilibrium: $\|\mathbf{p}'_{c(i)} - \mathbf{R}\mathbf{p}_i - \mathbf{t}\| \leq \|\mathbf{p}''_{c(i)} - \mathbf{R}\mathbf{p}_i - \mathbf{t}\|$ where $\mathbf{p}''_{c(i)}$ is an alternative of $\mathbf{p}'_{c(i)}$? To answer these useful and interesting questions, the investigation of the dynamics in the iterative process for automatic overlapping range image matching is necessary and may be encouraged.

Accurate matching often leads one range image to superimpose perfectly onto the other in 3D space, as demonstrated by the valve, dinosaur, and adapter images. Inaccurate matching often results in one range image either intersecting the other in 3D space, as demonstrated by the frog, cow, agpart, curvblock, and occl images, or sliding over the other in 3D space, as demonstrated by the buddha, duck, tubby, lobster, and cap images. This is because the cow images were cluttered by the background, the curvblock was occluded by an adapter, and the tubby images were captured from side views, while the buddha, duck, frog, lobster, and cap images include relatively simple geometry that can hardly uniquely pose the matching problem and deliver the camera motion information without any ambiguity. In this case, all the possible correspondences established using the traditional CPC must be meticulously manipulated, as is the case for the proposed EvolICP algorithm. Otherwise, the algorithms can easily converge pre-maturely or even diverge, yielding inaccurate matching results.

The deterministic annealing scheme is excellent for the global optimisation of the state variables even though it cannot guarantee (Puzicha et al. 1997) that the global minimum of the objective function is always found. In practice, the local minimum found by the deterministic annealing scheme often produces good matching results. For effective deterministic annealing, a sensible objective function must be constructed. This objective function is often data and context dependent. The minimum, maximum, and increasing rate of the inverse temperature must be carefully determined. While too large a maximum inverse temperature often leads matching algorithms to diverge, too large an inverse temperature increasing rate often leads matching algorithms to converge pre-maturely. Both cases usually lead to inaccurate matching results.

While the replicator equation is quite promising for modelling the dynamics in the iterative process of automatic overlapping range image matching, more experimental and theoretical studies will be conducted so that a clearer insight can be obtained into the probability estimation of possible correspondences established using the traditional CPC. If so, then the behaviour of overlapping range image matching algorithms can be predicted even before the matching process actually takes place. In this respect, we can learn from evolutionary biology and game theory.

Our work may promote the research on interactive game and mathematical biology theory in the sense of how to define fitness, how to differentiate between different individuals interacting with each other and competing for limited resources, and how to globally optimize the evolution of the entire population. The EvolICP algorithm proposed in this paper thus may provide a useful tool for interactive game and mathematical biology researchers to examine their theoretical analysis results over a finite population.

5.2 Conclusions

As far as we are aware, this is the first time ever that the automatic iterative overlapping range image matching process has been treated as an artificial evolutionary system and the widely used replicator equations in evolutionary biology and interactive game theory (Novak and Sigmund 2004; Stadler and Stadler 2003) have been then adapted for the modelling of its dynamics for accurate and robust matching results. Each image is represented as a limited number of discrete points. A point in one range image has different probabilities as possible replicators of points in another. The iterative matching process is discrete. After each iteration, the possible correspondences have to be re-established. Since the replicator equation assumes infinite population size, complete mixture of strategies, time continuous process, and true breeding organisms that violate the actual conditions of the iterative discrete range image matching process, the adaptation is compulsory. While it is often difficult to determine the payoff matrix, resulting in biological and game evolutions being somewhat aimless and unpredictable, the range image matching process has a clear target range image to evolve towards. The adaptation has been implemented from the following five aspects:

- While the replicator equations use the absolute fitness difference, the proposed EvolICP algorithm has used the relative fitness difference instead to describe the probability change of each individual in the population being a point in the overlapping area over successive iterations;
- While the replicator equations often define subjectively or in a subtle way the fitness of individuals in the population for problem investigation in the evolutionary process of interactive game and mathematical biology, the proposed EvolICP algorithm has defined the fitness of the individuals as the negative of a power of the SEDs between their resulting possible correspondences established using the traditional CPC;

- While the replicator equation penalizes those individuals with low fitness, the proposed EvolICP algorithm has further penalised them with an attempt to eventually reduce the average matching error over the entire population;
- While the replicator equations allow different strategies in the population to be chosen by an arbitrary number of players, the proposed EvolICP algorithm has penalised with an attempt to differentiate real correspondences from false ones those individuals in one image that select the same points in another as their possible replicators; and finally
- After the probabilities of possible correspondences established using the traditional CPC have been estimated by the replicator equation, they have been embedded into the powerful deterministic annealing scheme for global optimization.

From all the experimental results presented in this paper, which were all based on real range images, it can be concluded that the replicator equations have been successfully adapted to characterise the dynamics of the iterative process for automatic overlapping range image matching, resulting in accurate and stable results. The proposed EvolICP algorithm on the whole outperforms either the SoftICP, GenICP, ICP3, GA, or LSP algorithm for the automatic matching of overlapping range images in the sense of accuracy and robustness with regard to image complexities, orders, resolutions, noise characteristics, etc. Even though it is challenging to match images captured from side views, cluttered by the background, or occluded by other objects, the proposed EvolICP algorithm could still match them successfully.

Comparing the proposed EvolICP algorithm with the classification based matching method (Zhang 1992; Pulli 1999; Turk and Levoy 1994; Liu et al. 2000), the former is advantageous for range image matching. While the latter is based on ad hoc heuristics, the former provides a clear insight into the dynamics of the iterative range image matching process, deepening our understanding of how to accurately estimate and optimize the state variables. Such insight is critical for the development of advanced overlapping range image matching algorithms. Comparing the proposed EvolICP algorithm with the existing probability based method (Gold et al. 1998; Dewaele et al. 2004; Granger and Pennec 2002), the latter usually assumes that the average matching error of the entire population is zero, treats equally all possible correspondences established and has to explicitly model outliers, whilst the former explicitly takes the average matching error into account and penalises those individuals with low fitness or competing for the same points as their possible replicators without the need of explicit outlier modelling. While explicit outlier modelling may artificially interfere the evolution, the former lets the evolutionary process itself determine which individual in the population will expand or shrink. Clearly, the former describes more realistic scenarios and thus, often produces more accurate and robust matching results. The replicator equations are usually more effective than either the Shannon or Tsallis entropy for the description of the dynamics in the automatic iterative overlapping range image matching process.

Compared with either the GA or LSP algorithm, the proposed EvolICP algorithm represents a different and usually more effective strategy for overlapping range image matching and has an advantage of easy implementation. It is hard for the GA to always successfully find the globally optimal camera motion parameters within predictable time and for the LSP method to directly establish real point matches between overlapping range images. In contrast, it is usually straightforward for the proposed EvolICP algorithm to evolve the probabilities of possible correspondences being real, usually yielding decent registration results.

Further research includes improving the computational efficiency and theoretically investigating the behaviour of the proposed EvolICP algorithm for the automatic matching of various overlapping range images. For the former, the camera motion interpolation and salient point detection may be employed. For the latter, the knowledge from evolutionary biology and interactive game theory (Alboszta and Miekisz 2004; Pykh 2005) about how to construct the Lyapunov function and how to establish ESS and equilibrium can be learned. For accuracy and robustness, genetic operators (crossover, mutation, etc.) may be inserted into the proposed EvolICP algorithm for even better automatic overlapping range image matching results.

Acknowledgements We would like to express our sincere thanks to both the anonymous editor and reviewers for their thoughtful comments that have improved the quality of the paper. Thanks also go to Dr Lynda Thomas, Dr Edel Sherratt and John T. Roberts from Aberystwyth University for their proofreading that has improved the readability of the paper.

References

Alboszta, J., & Miekisz, J. (2004). Stability of evolutionarily stable strategies in discrete replicator dynamics with time delay. *Journal Theoretical Biology*, *231*, 175–179.

Allen, P. K., Stamos, I., Troccoli, A., Smith, B., Leordeanu, M., & Hsu, Y. C. (2003). 3D modelling of historic sites using range and image data. In *Proceedings of ICRA* (pp. 145–150) 2003.

Andreetto, M., Brusco, N., & Cortelazzo, G. M. (2004). Automatic 3D modelling of textured cultural heritage objects. *IEEE Transactions Image Processing*, *13*, 354–369.

Ashbrook, A. P., Fisher, R. B., Robertson, C., & Werghi, N. (1998). Finding surface correspondences for object recognition and registration using pair-wise geometric histogram. In *Proceedings of the 5th ECCV* (Vol. II, pp. 185–201) 1998.

Besl, P. J., & McKay, N. D. (1992). A method for registration of 3D shapes. *IEEE Transactions on Pattern Analysis and Machine Intelligence*, *14*, 239–256.

Brusco, N., Andreetto, M., Carmignato, S., & Cortelazzo, G. M. (2004). Metrological analysis of a procedure for the automatic 3D modelling of dental plaster casts. In *Proceedings of 3DPVT* (pp. 592–599) 2004.

Brusco, N., Andreetto, M., Giorgi, A., & Cortelazzo, G. M. (2005). 3D registration by textured spin-images. In *Proceedings of the 3DIM* (pp. 262–269) 2005.

Chang, M., Leymarie, F. F., & Kimia, B. B. (2004). 3D shape registration using regularized medial scaffolds. In *Proceedings of 3DPVT* (pp. 987–994) 2004.

Chen, H., & Bhanu, B. (2007). 3D free form object recognition in range images using local surface patches. *Pattern Recognition Letters*, *28*, 1252–1262.

Chen, Y., & Medioni, G. (1992). Object modelling by matching of multiple range images. *Image and Vision Computing*, *10*, 145–155.

Chen, C.-S., Hung, Y.-P., & Cheng, J. B. (1999). RANSAC-based DARCES: a new approach to fast automatic registration of partially overlapping range images. *IEEE Transactions on Pattern Analysis and Machine Intelligence*, *21*, 1229–1234.

Dewaele, G., Devernay, F., & Horaud, R. (2004). Hand motion from 3D point trajectories and a smooth surface model. In *Proceedings of ECCV* (pp. 495–507) 2004.

Dorai, C., & Wang, G. (1998). Registration and integration of multiple object views for 3D model construction. *IEEE Transactions on Pattern Analysis and Machine Intelligence*, *20*, 83–89.

Fisher, R. A. (1930). *The genetical theory of natural selection*. Oxford: Clarendon Press.

Friedman, J. H., Bently, J. L., & Finkel, P. A. (1977). An algorithm for finding best matches in logarithmic expected time. *ACM Transactions on Mathematical Software*, *3*, 209–226.

Gold, S., & Rangarajan, A. (1996). A graduated assignment algorithm for graph matching. *IEEE Transactions on Pattern Analysis and Machine Intelligence*, *18*, 377–388.

Gold, S., Rangarajan, A., Lu, C.-P., Pappu, S., & Mjolsness, E. (1998). New algorithms for 2-D and 3-D point matching: pose estimation and correspondence. *Pattern Recognition*, *31*, 1019–1031.

Granger, S., & Pennec, X. (2002). Multi-scale EM-ICP: a fast and robust approach for surface registration. In *Proceedings of ECCV* (pp. 418–432) 2002.

Huber, D., & Hebert, M. (2003). Fully automatic registration of multiple 3D data sets. *Image and Vision Computing*, *23*, 637–650.

Johnson, A., & Hebert, M. (1999). Using spin images for efficient object recognition in cluttered 3D scenes. *IEEE Transactions on Pattern Analysis and Machine Intelligence*, *21*, 433–449.

Liu, Y. (2005). Automatic range image matching using the graduated assignment algorithm. *Pattern Recognition*, *38*, 1615–1631.

Liu, Y. (2006). Automatic registration of overlapping 3D point clouds using closest points. *Image and Vision Computing*, *24*, 762–781.

Liu, Y., & Wei, B. (2004). Developing structural constraints for accurate registration of overlapping range images. *Robotics and Autonomous Systems*, *47*, 11–30.

Liu, Y., Rodrigues, M. A., & Wang, Y. (2000). Developing rigid motion constraints for the registration of free-form shapes. In *Proceedings of IROS* (pp. 2280–2285) 2000.

Liu, Y., Wei, B., Li, L., & Zhou, H. (2006a). Projecting registration error for accurate registration of overlapping range images. *Robotics and Autonomous Systems*, *54*, 428–441.

Liu, Y., Zhou, H., Su, X., Ni, M., & Lloyd, R. J. (2006b). Transforming least squares to weighted least squares for accurate range image registration. In *Proceedings of 3DPVT* (pp. 232–239) 2006.

Lomonosov, E., Chetverikov, D., & Ekart, A. (2006). Pre-registration of arbitrarily oriented 3D surfaces using a genetic algorithm. *Pattern Recognition Letters*, *27*, 1201–1208.

Makadia, A., Patterson IV, A., & Daniilidis, K. (2006). Fully automatic registration of 3D point clouds. In *Proceedings of CVPR* (pp. 1297–1304) 2006.

Novak, M. A., & Sigmund, K. (2004). Evolutionary dynamics of biological games. *Science*, *303*, 793–799.

Pajdla, T., & Van Gool, L. (1995). Matching of 3-D curves using semi-differential invariants. In *Proceedings of ICCV* (pp. 390–395) 1995.

Pelillo, M. (1999). Replicator equations, maximal cliques, and graph isomorphism. *Neural Computation*, *11*, 1933–1955.

Pulli, K. (1999). Multiview registration for large data sets. In *Proceedings of 3DIM* (pp. 160–168) 1999.

Puzicha, J., Hofmann, T., & Buhmann, J. M. (1997). Deterministic annealing: fast physical heuristics for real-time optimisation of large systems. In *Proceedings of 15th IMACS World Conference on Scientific Computation, Modelling and Applied Mathematics* (Vol. VI, pp. 445–450) 1997.

Pykh, Y. A. (2005). Direct Lyapunov method in the theory of replicator system with entropy-like applications. In *Proceedings of International Conference Physics and Control* (pp. 56–59) 2005.

Rusinkiewicz, S., & Levoy, M. (2001). Efficient variants of the ICP algorithm. In *Proceedings of 3DIM* (pp. 145–152) 2001.

Santamaria, J., Cordon, O., Damas, S., Aleman, I., & Botella, M. (2007). A scatter search-based technique for pair-wise 3D range image registration in forensic anthropology. *Soft Computing*, *11*, 819–828.

Schutz, C., Jost, T., & Hugli, H. (1998). Multi-feature matching algorithm for free-form 3D surface registration. In *Proceedings of ICPR* (pp. 982–984) 1998.

Sharp, G. C., Lee, S. W., & Wehe, D. K. (2002). ICP registration using invariant features. *IEEE Transactions on Pattern Analysis and Machine Intelligence*, *24*, 90–112.

Silva, L. (2005). Olga R.P. Bellon, and K.L. Boyer, Precision range image registration using a robust surface interpenetration measure and enhanced genetic algorithms. *IEEE Transactions on Pattern Analysis and Machine Intelligence*, *27*, 762–776.

Stadler, B. M. R., & Stadler, P. F. (2003). Molecular replicator dynamics. *Advances in Complex Systems*, *6*, 47–77.

Stewart, C. V., Tsai, C.-L., & Roysam, B. (2003). The dual-bootstrap iterative closest point algorithm with application to retinal image registration. *IEEE Transactions on Medical Imaging*, *22*, 1379–1394.

Turk, G., & Levoy, M. (1994). Zippered polygon meshes from range images. In *Proc. SIGGRAPH* (pp. 311–318) 1994.

Xiao, G., Ong, S. H., & Foong, K. W. C. (2007). 3D registration of partially overlapping surfaces using a volumetric approach. *Image and Vision Computing*, *25*, 934–944.

Yamany, S. M., & Farag, A. A. (2002). Surface signatures: an orientation independent free-form surface representation scheme for the purpose of objects registration and matching. *IEEE Transactions on Pattern Analysis and Machine Intelligence*, *24*, 1105–1120.

Zagorchev, L., & Goshtasby, A. (2005). A mechanism for range image integration without image registration. In *Proceedings of 5th 3DIM* (pp. 126–133) 2005.

Zhang, Z. (1992). *Iterative point matching for registration of free-form curves* (Technical report, No. 1658). INRIA, France.

Zhao, W., Nister, D., & Hsu, S. (2004). Alignment of continuous video onto 3D point clouds. In *Proceedings of CVPR* (pp. 964–971) 2004.

Zhu, L., Barhak, J., Srivatsan, V., & Katz, R. (2007). Efficient registration for precision inspection of free-form shapes. *International Journal of Advanced Manufacturing Technology*, *32*, 505–515.